NASA/CR—2014-218112

Multi-Point Combustion System
Final Report

Jerry Goeke, Spencer Pack, Gregory Zink, and Jason Ryon
UTC Aerospace Systems,West Des Moines, Iowa

April 2014

NASA STI Program . . . in Profile

Since its founding, NASA has been dedicated to the advancement of aeronautics and space science. The NASA Scientific and Technical Information (STI) program plays a key part in helping NASA maintain this important role.

The NASA STI Program operates under the auspices of the Agency Chief Information Officer. It collects, organizes, provides for archiving, and disseminates NASA's STI. The NASA STI program provides access to the NASA Aeronautics and Space Database and its public interface, the NASA Technical Reports Server, thus providing one of the largest collections of aeronautical and space science STI in the world. Results are published in both non-NASA channels and by NASA in the NASA STI Report Series, which includes the following report types:

- TECHNICAL PUBLICATION. Reports of completed research or a major significant phase of research that present the results of NASA programs and include extensive data or theoretical analysis. Includes compilations of significant scientific and technical data and information deemed to be of continuing reference value. NASA counterpart of peer-reviewed formal professional papers but has less stringent limitations on manuscript length and extent of graphic presentations.

- TECHNICAL MEMORANDUM. Scientific and technical findings that are preliminary or of specialized interest, e.g., quick release reports, working papers, and bibliographies that contain minimal annotation. Does not contain extensive analysis.

- CONTRACTOR REPORT. Scientific and technical findings by NASA-sponsored contractors and grantees.

- CONFERENCE PUBLICATION. Collected papers from scientific and technical conferences, symposia, seminars, or other meetings sponsored or cosponsored by NASA.

- SPECIAL PUBLICATION. Scientific, technical, or historical information from NASA programs, projects, and missions, often concerned with subjects having substantial public interest.

- TECHNICAL TRANSLATION. English-language translations of foreign scientific and technical material pertinent to NASA's mission.

Specialized services also include creating custom thesauri, building customized databases, organizing and publishing research results.

For more information about the NASA STI program, see the following:

- Access the NASA STI program home page at *http://www.sti.nasa.gov*

- E-mail your question to *help@sti.nasa.gov*

- Fax your question to the NASA STI Information Desk at 443–757–5803

- Phone the NASA STI Information Desk at 443–757–5802

- Write to:
  STI Information Desk
  NASA Center for AeroSpace Information
  7115 Standard Drive
  Hanover, MD 21076–1320

NASA/CR—2014-218112

Multi-Point Combustion System
Final Report

Jerry Goeke, Spencer Pack, Gregory Zink, and Jason Ryon
UTC Aerospace Systems,West Des Moines, Iowa

National Aeronautics and
Space Administration

Glenn Research Center
Cleveland, Ohio 44135

April 2014

Acknowledgments

This report contains preliminary findings,
subject to revision as analysis proceeds.

Level of Review: This material has been technically reviewed by NASA technical management OR expert reviewer(s).

Multi-Point Combustion System
Final Report

Jerry Goeke, Spencer Pack, Gregory Zink, and Jason Ryon
UTC Aerospace Systems
West Des Moines, Iowa 50265

Abstract

A low-NOx emission combustor concept has been developed for NASA's Environmentally Responsible Aircraft (ERA) program to meet N+2 emissions goals for a 70,000 lb thrust engine application. These goals include 75 percent reduction of LTO NOx from CAEP6 standards without increasing CO, UHC, or smoke from that of current state of the art. An additional key factor in this work is to improve lean combustion stability over that of previous work performed on similar technology in the early 2000s. The purpose of this paper is to present the final report for the NASA contract. This work included the design, analysis, and test of a multi-point combustion system. All design work was based on the results of Computational Fluid Dynamics modeling with the end results tested on a medium pressure combustion rig at the UC and a medium pressure combustion rig at GRC. The theories behind the designs, results of analysis, and experimental test data will be discussed in this report. The combustion system consists of five radially staged rows of injectors, where ten small scale injectors are used in place of a single traditional nozzle. Major accomplishments of the current work include the design of a Multipoint Lean Direct Injection (MLDI) array and associated air blast and pilot fuel injectors, which is expected to meet or exceed the goal of a 75 percent reduction in LTO NOx from CAEP6 standards. This design incorporates a reduced number of injectors over previous multipoint designs, simplified and lightweight components, and a very compact combustor section. Additional outcomes of the program are validation that the design of these combustion systems can be aided by the use of Computational Fluid Dynamics to predict and reduce emissions. Furthermore, the staging of fuel through the individually controlled radially staged injector rows successfully demonstrated improved low power operability as well as improvements in emissions over previous multipoint designs. Additional comparison between Jet-A fuel and a hydrotreated biofuel is made to determine viability of the technology for use with alternative fuels. Finally, the operability of the array and associated nozzles proved to be very stable without requiring additional active or passive control systems. A number of publications have been published pertaining to the current effort as well as three patent applications which have been submitted.

Summary

In response to NASA's solicitation for Research and Development of Low-Emissions Combustor Concepts and Associated Fuel Control Valves, Delavan Inc. doing business as Turbine Fuel Technologies (TFT), now part of the Engine Components division of UTC Aerospace Systems provided a proposal for a radially staged Multi-Point Lean Direct Injection (MLDI) combustion system. The goal of this program was to use Multipoint Lean Direct Injection technology to demonstrate NOx reduction of 75 percent of the CAEP 6 recommendations in an advanced gas turbine combustor environment. The work began with review of prior art and lessons learned by TFT and NASA on MLDI systems and culminated in successful completion of medium pressure combustion rig testing at NASA Glenn Research Center (GRC). Along the way TFT evaluated over one hundred design iterations using Computational Fluid Dynamics (CFD), conducted high temperature single injector testing at TFT, and performed medium pressure rig testing at the University of Cincinnati (UC).

Experimental results of the program included lean blow out (LBO) at average fuel air ratios (FAR) of 0.0046 (equivalence ratio, ϕ=0.0676) using Jet-A fuel and FAR=0.0044 (ϕ=0.0647) using hydrotreated biofuel. These tests were conducted at the UC at a Combustor Inlet Pressure, P3 of 55 psia, Combustor

Inlet Temperature, T3 of 434 °F and a 4 percent ΔP drop across the combustor. Testing at NASA's CE-5 combustion rig resulted in best case EINOx at take-off conditions of less than 4 g-NOx/kg-fuel. All of the testing to date indicates that this system has acceptable levels of stability without any additional active or passive control. Evaluation of previous NASA emissions data indicates that 75 percent reduction in CAEP 6 NOx would equate to a maximum EINOx of 27 g-NOx/kg-fuel at an associated engine takeoff condition for a 55:1 pressure ratio engine. Extrapolation of rig test data indicates the MLDI system should provide an EINOx of 26.8 g-NOx/kg-fuel at a FAR=0.035 and a 55:1 pressure ratio. Thus this system is expected to meet, or exceed the objectives of this program. It is also expected that minor changes to the system that was tested would result in significant reductions in the emissions test results. These changes include reducing the percentage of fuel into the pilot injectors with a corresponding increase in fuel to the outer air blast injectors and reducing air leakage around the combustor dome.

Progress Summary

The contract for this program was signed on March, 18, 2011. Subsequently, Turbine Fuel Technologies, Goodrich Corp. (TFT or Goodrich) now United Technologies Aerospace Systems (UTAS), began a detailed review of papers and presentations published on previous multi-point combustion work. Based on this work and TFT's proposal, a preliminary concept was sketched. The historical perspective and the preliminary concept were presented to NASA as part of a contract kick-off and collaboration meeting on April 8, 2011.

TFT began initial designs of the multi-point injectors shortly after the meeting at NASA. This work included refining the initial combustion concept and creating target fuel and air flows for each of the injector circuits. This original concept included the use of pressure atomizing fuel injectors for all of the fuel circuits. Computational Fluid Dynamics analysis was utilized to help guide the process of selecting appropriate fuel injectors. Preliminary engine flight conditions were finalized in May 2011 after receipt of engine conditions from NASA.

Review of CFD data for arrays of pressure atomizing injectors indicates that the concentrated fuel flow through these injectors may result in higher levels of emissions than preferred, especially at higher operating pressure ratios. In order to reduce the impact of the large fuel flows, TFT investigated the use of air blast fuel injectors for the intermediate injectors and outer fuel injectors. CFD results for these configurations indicate a more homogeneous temperature distribution at the outlet of the combustor along with reduced hot spots near the injectors as compared to an all pressure atomizer array and a substantial improvement in predicted EINOx.

An extensive amount of CFD analysis was completed for both pressure atomizer and air blast fuel injectors in the single injector rig and for injector array variations. The result of these analyses provided TFT with comparative data on variations in the system design which was utilized to down select specific designs for rig testing. A status review was held at GRC on October 18, 2011, where all CFD analysis, the proposed testing, and a program status review were presented. Subsequent to this meeting, TFT continued to refine the air blast design with design iterations driven by CFD estimates of the temperature profiles and EINOx estimates, and developed a concept which shows great promise.

In addition to concepts and analysis for the injectors, design and manufacture of a single injector test rig was completed. The single injector test rig was designed for air temperatures in excess of 900°F at ambient pressures. This rig was utilized to test nine different pressure atomizing and three different air blast atomizing single injector assemblies. Analysis of the test results indicated acceptable operation of the pressure atomizing nozzles that were previously selected for further testing based on CFD results. However, there was some concern regarding unsteady operation of early air blast atomizer concepts which led to further development of these designs. The air blast atomizers were also tested using R-8 biofuel which provided similar results as those for Jet-A fuel.

Design, drafting, and manufacturing of a combustion rig test assembly for testing injector arrays was completed. This rig was designed for use at ambient through medium pressure so that the same rig could be used for testing at TFT as well as at the UC. The first set of tests at the UC was completed in early

May 2012 using an array consisting entirely of pressure atomizing fuel injectors with air assist swirlers. Lean blow out tests and some tests at idle conditions were conducted using Jet-A fuel and R-8 biofuel. These tests resulted in an average LBO or weak extinction fuel to air ratio, FAR=0.00292 (ϕ=0.043) for Jet-A and FAR=0.00231 (ϕ=0.034) for R-8 fuel. This data is slightly higher than the LBO of single pilot injectors which would be expected for testing at a higher pressure.

A second set of tests was conducted at UC in August of 2012 using air-blast atomizing injectors for intermediate and outer positions in place of the pressure atomizing injectors used in the previous tests. The pressure atomizer pilot injectors remained the same as in the previous test. This testing included idle, LBO, and some off idle testing. Idle and LBO tests were conducted on both Jet-A fuel and R-8 biofuel. All scheduled testing was completed satisfactorily within the test time frame. Data from the tests indicate an average LBO or weak extinction FAR=0.0046 (ϕ=0.068) for Jet-A and FAR=0.0045 (ϕ=0.066) for R-8 fuel. Both tests were conducted starting from idle conditions (P3=55 psia, 4 percent ΔP, T3=434 °F) using only the pilot fuel injectors. Testing demonstrated operability of the very lean air-blast system for the first time. In addition to the lean limits, the pilot injectors were stable at very lean power conditions, operating at T3=600 °F and FAR=0.035.

Hardware for the tests continued to be tested at the UC so that their PhD students could continue to test the system and use this experience to continue to improve the accuracy of their emissions measurement system. After numerous tests, the sides of the rig test combustor became too warped to safely continue the testing and the rig was returned to TFT for repair. These repairs were completed in April of 2013 and the rig was returned to UC for additional testing.

In September of 2012, the TFT team completed assembly and shipped the CE-5 rig test hardware to NASA. Testing of this assembly was scheduled for the week of October 22, 2012, along with a status review at GRC. The attempt to conduct rig testing was discontinued due to damage to the fuel injectors. After receipt of the rig test articles in our facility, TFT conducted a full investigation into the root cause of the damage and concluded that exposure of the o-rings to temperatures in excess of 600 °F without fuel flow resulted in complete failure of the seals. All analysis conducted prior to, and after, the o-ring failure indicated that the o-rings would have functioned as intended if fuel had been flowing through the pilot circuit during the temperature excursion to 1000 °F.

Subsequent to this testing, Turbine Fuel Technologies redesigned the rig assembly to eliminate the o-rings in the fuel manifold. This work was completed in January 2013 with piece part manufacturing completed in February and all subassemblies completed in March 2013. Final assembly and test was conducted in April and the final assembly was shipped to NASA for testing in the CE-5 rig.

In addition to these tasks, a new pilot design was developed in February of 2013. The new design, based off of performance development and atmospheric burn rig testing, was expected to improve the LBO capability of the system while reducing unburnt hydrocarbons. Preliminary CFD analysis of the system with the new pilot indicates that the new design would not adversely impact the emissions of the system at full power.

Final testing in NASA's CE-5 rig was conducted in late May of 2013. Goodrich was allowed three days to complete the testing. Best case results from these tests were an EINOx at cruise conditions of 3.02 g-NOx/kg-fuel and EINOx of 4.0 g-NOx/kg-fuel at simulated take-off conditions. It is expected that additional testing could have improved upon these test results given the chance to vary fuel splits.

Detailed Progress Report

Figure 1 is a picture of the initial concept for the Goodrich multi-point combustion system while Figure 2 shows the arrangement from the combustor looking upstream. These figures are included as a reference for comparison to Figure 3 which shows the array with air blast atomizers.
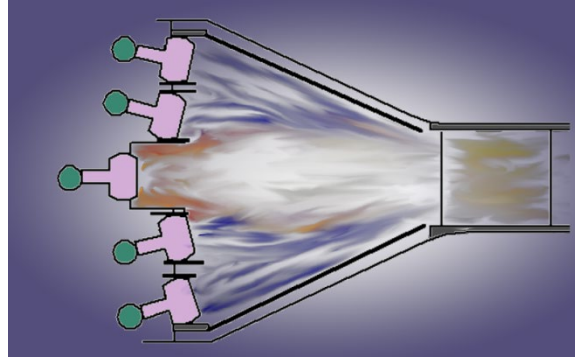
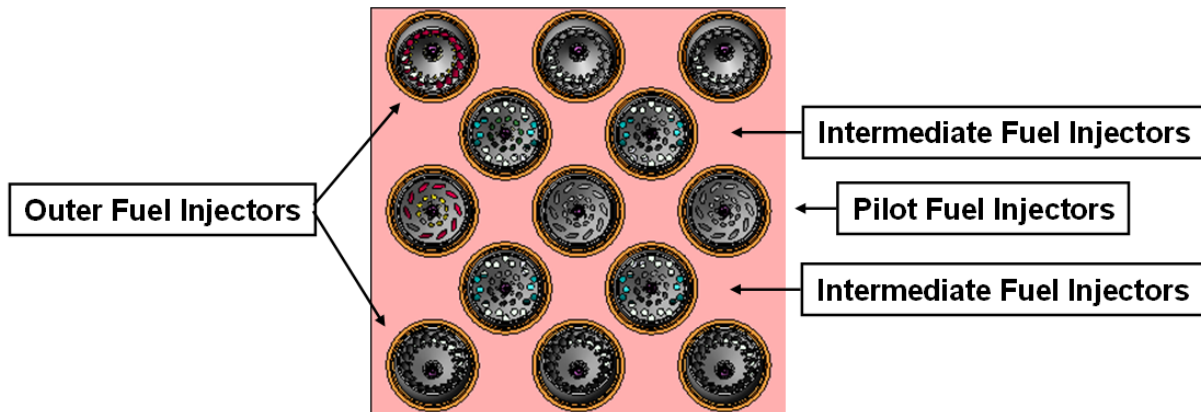Figure 1.—Multi-Point Concept.

Figure 2.—Multi-Point Array with pressure atomizer fuel injectors.

Figure 3.—Multi-Point Array with air blast fuel injectors.

Computational Fluid Dynamics (CFD) was used extensively in the preliminary design of the array as well as the individual fuel injectors. Initially, CFD was used to determine the inter-nozzle mixing characteristics of the array as well as mapping the recirculation zones. An example of this type of simulation is shown below in Figure 4 which shows the interaction between nozzles as well as the convergence of the combustor section mix out the large scale velocity characteristics as the flow reaches the exit of the combustor.
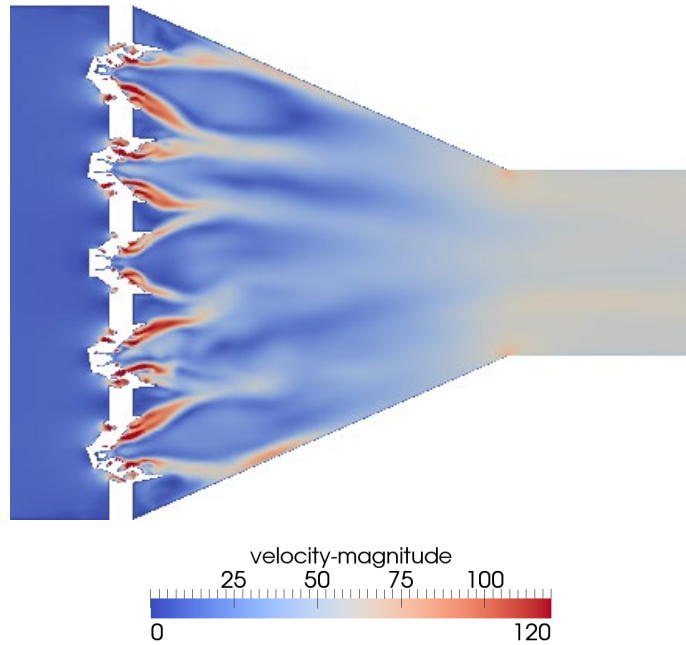
Figure 4.—CFD velocity contours (air-only) showing mixing characteristics of the original pressure atomizer array concept.
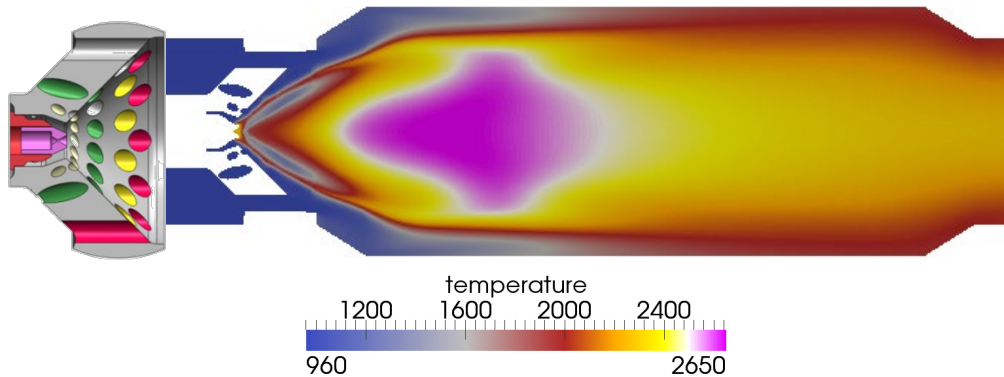

Figure 5.—CFD temperature profile of an early pressure atomizer concept.

As the program developed, reacting CFD simulations were used to predict the NOx emissions of individual nozzles and of the entire array. With NOx as a key parameter, the design of the individual atomizers was further developed with the intent of designing atomizers that would achieve low NOx targets. The use of this CFD determined that the pressure atomizers envisioned at the beginning of the program would not be capable of adequately mixing the fuel and air which is required to achieve the aggressive low NOx targets, particularly at the high operating pressure ratio conditions (see Figure 5).

These analyses provided the insight needed to develop air blast atomizers for the array which would be better capable of distributing the fuel and air at the local injector level. The development of the high-shear air blast injectors for use in the array (patent pending U.S. 13/665,497, U.S. 13/665,568) was shown by CFD to indeed lower the predicted NOx to less than 15 percent of the NOx that was originally predicted to be produced by the original pressure atomizers. In total, over 100 nozzle configurations were simulated in order to arrive at a go-forward concept, which is shown in Figure 6. Values of the predicted EINOx are provided in Table 1.
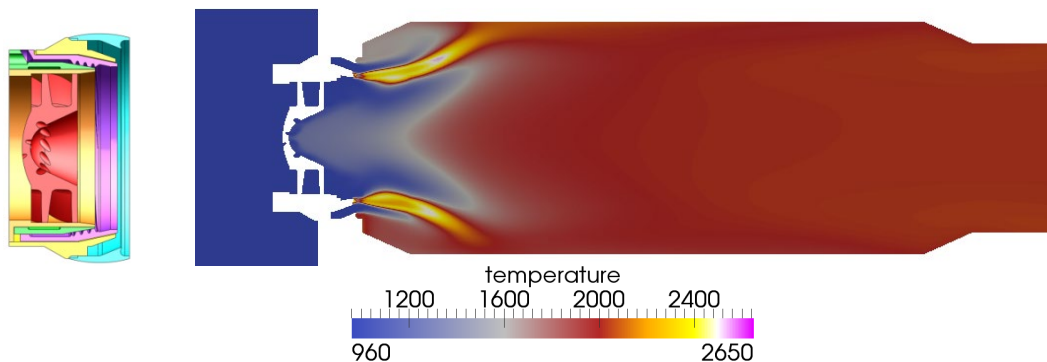
Figure 6.—CFD temperature profile of an air-blast atomizer.

TABLE 1.—CFD PREDICTIONS OF EINOx

	P3, psi	T3, °F	Equivalence ratio, ϕ	CFD predicted EINOx, g-NOx/kg-fuel
Rig match point	250	1000	0.368	5.02
Design point	809	1269	.515	26.89

Two variations of this injector are used in the hardware for all rig testing. They employ identical fuel circuits, and the only difference is a slightly larger effective area, ACd = 0.1875 in^2 for the intermediate nozzles in the array compared to the outer nozzles which has ACd = 0.1500 in^2. These injectors have approximately 40 percent of the air through the highly swirling center air circuit, with the remaining balance of air through a minimally swirling outer air circuit. The fuel is delivered along a short prefilmer which allows the inner air to circumferentially spread the fuel prior to it entering a very high shear zone caused by the difference in the inner and outer swirl strengths. The minimally swirling outer air circuit combined with the high swirl inner circuit provide for an aerodynamic confinement which promotes the thorough and rapid mixing of fuel and air within a very short distance from the nozzle. Additionally, downstream of the fuel mixing zone, the swirl from the inner air circuit prevails over the minimally swirling outer zone, retaining a high amount of overall swirl in the injector, which allows it to mix with other injectors in the full multipoint array.

CFD was further utilized to predict the NOx associated with the interaction of these nozzles within in the converging combustor in the array, with one such simulation shown in Figure 7. The simulations modeled the entire multipoint array and showed both the local nozzle mixing zones where the fuel and air are quickly mixed and reacted, as well as the inter-nozzle mixing zones as the residual swirl from the nozzles combined with the convergence of the combustor result in a uniform temperature distribution. The overall NOx predicted by these simulations tracks very closely to the individual nozzle predictions. Most noticeably, the pilot nozzles, which are still pressure atomizers, produce higher levels of NOx per pound of fuel compared to the intermediate and outer nozzles, which are air blast injectors. Further analyses were used to simulate the effects of adjusting the fuel to independently staged manifolds, and it was found that by reducing the local fuel to air ratio of the pilot stage while increasing the fuel to air ratio of the intermediate and outer nozzles, that the NOx was able to be further reduced to exceed the goal of 75 percent reduction in LTO NOx below CAEP 6. This insight of independently staging the fuel circuits was used to develop the basis for the rig test strategy. Additionally, the CFD predicts the array to meet the target EINOx at the original design point at a 55:1 pressure ratio.
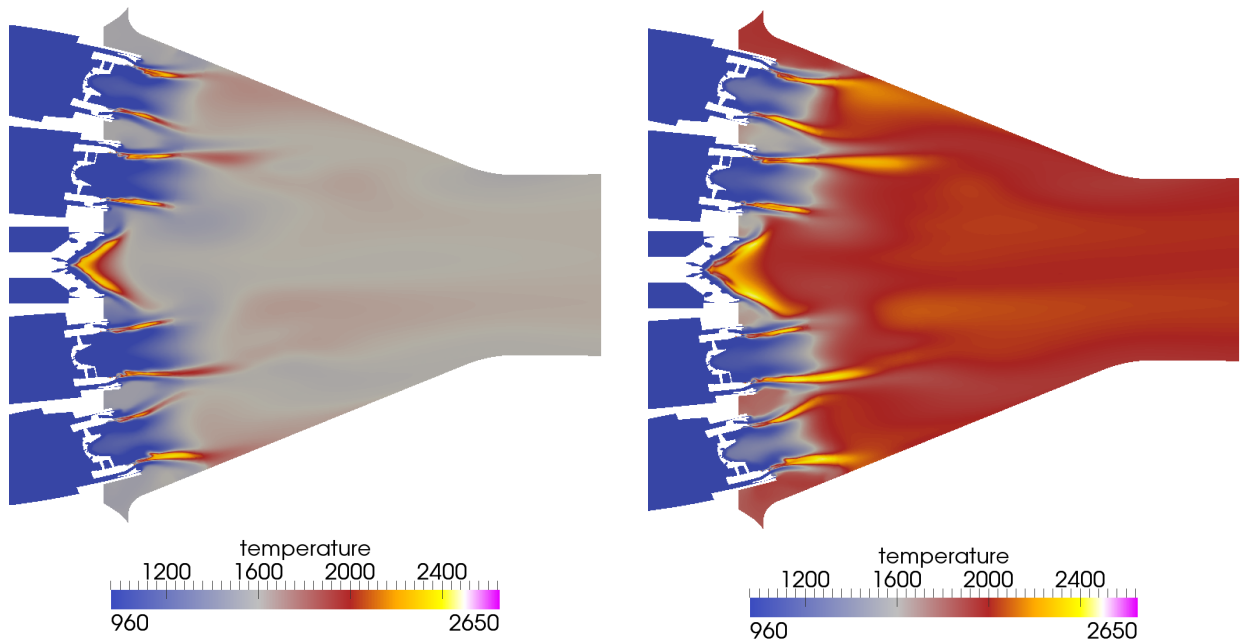
Figure 7.—CFD temperature profiles of the airblast array at the Rig Match Point (left) and the Design Point (right).

Figure 8.—MLDI combustor installed in the UC rig.

Intermediate rig testing was started on April 30, 2012, with installation of the combustor and fuel injectors as shown in Figure 8. Figure 8 shows the combustor in an upstream view prior to closing the combustion rig's pressure vessel. Figure 9 is a close-up of the combustor showing fuel injectors in the MLDI array while Figure 10 is a picture of the injectors taken upstream of the combustor.

Lean blow out tests were conducted on this rig using Jet-A fuel and R-8 biofuel. These tests resulted in an average LBO or weak extinction FAR=0.00292 (ϕ=0.043) for Jet-A and FAR=0.00231 (ϕ=0.034) for R-8 fuel. The data from these tests is in Table 2.
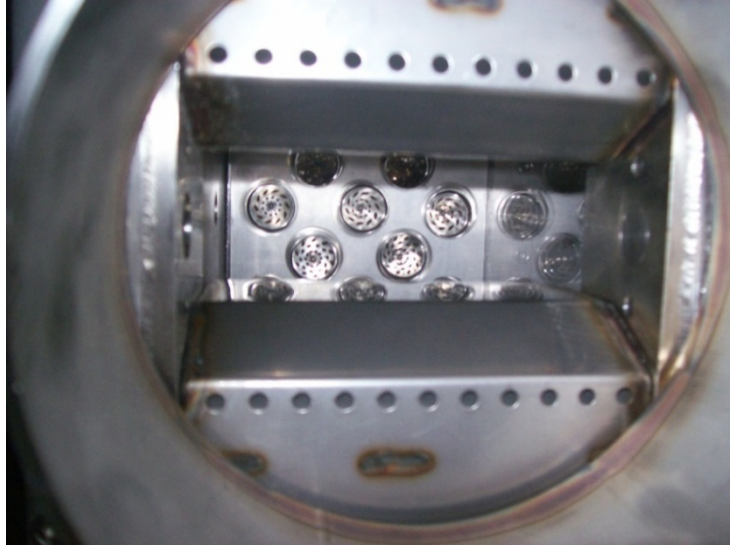
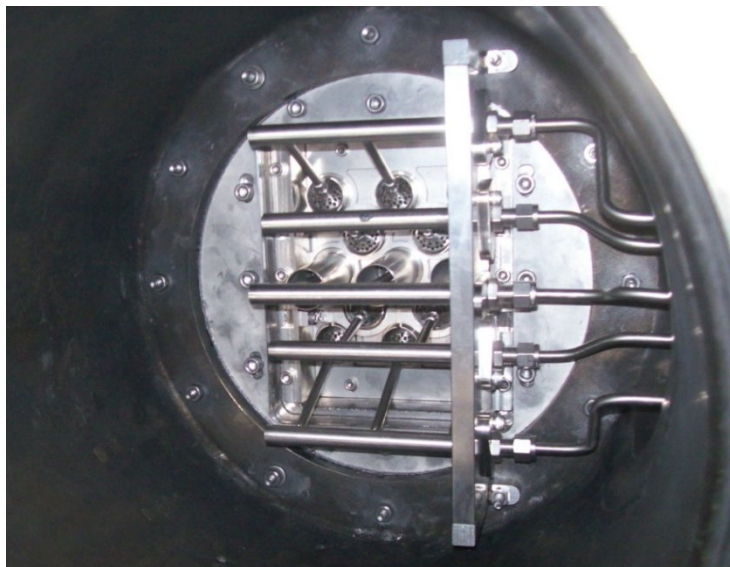Figure 9.—Close-up of MLDI Combustor installed in the UC rig.

Figure 10.—MLDI injectors installed in the UC rig.

TABLE 2.—UC LBO TEST DATA

Fuel	Test no.	P3, psi	T3, °F	ΔP, %	ϕ
Jet-A	LBO 1	55.50	433	1.874	0.044
	LBO 2	55.65	433	1.905	0.042
	LBO 3	55.63	433	1.887	0.044
R-8 fuel	LBO 1	55.90	434	1.914	0.033
	LBO 2	56.08	431	2.015	0.034
	LBO 3	56.15	434	1.959	0.034

The next set of rig tests at the UC was for idle conditions. These tests resulted in data that is suspect due to the set points for test conditions being calculated based on a ΔP of 4 percent and UC was not able to reach 4 percent ΔP and instead ran at 2 percent without reducing the fuel flow. This resulted in conditions that were exceptionally rich. In addition, testing indicates a large amount of air leakage around the dome plate which may have contributed to increasing the localized richness of the fuel.

All tests running pilot only as well as a combination of the pilot and intermediate injectors appeared to be stable. However, it was difficult to keep all three circuits lit when all three (pilot, intermediate, and outer) fuel circuits were used unless the fuel flow was increased beyond the intended fuel air ratio in order to keep both the pilot and the main lit. Otherwise, either set of injectors would blow out.

Rig testing was halted after experiencing some uncharacteristic instability on the rig. Subsequent fuel shut-down resulted in an extended burn of fuel even though fuel was not being delivered to the rig. Inspection of the rig indicated the dome plate was warped. Low pressure burn confirmed fuel was leaking under the dome plate, collecting, and burning around the plate. Subsequent air flow testing measured an air effective area of 3.53 in^2 for this assembly. CFD of the injector assembly indicates a target air effective area of 2.0 in^2. The discrepancy in the actual versus the calculated air effective area indicates a very large amount of air leakage around the dome plate.

TFT redesigned the dome plate to reduce air leakage, replaced the intermediate and outer injectors with air blast atomizers, reassembled the rig, and returned for additional testing at the UC. Cold flow testing of this assembly prior to delivery of the parts to UC measured a new air effective area of 2.17 in^2, which is indicative of a small amount of air leakage. Actual results during testing indicated an average air effective area of 1.75 in^2 which demonstrated successful resolution of this problem as well as a tight fit when the components are heated to running conditions. A view of the three dimensional model of the new air blast array and the new dome plate installed in the medium pressure rig assembly is shown in Figure 11. This design change, along with replacing an air valve at the UC allowed the combustion rig to reach the required 4 percent ΔP across the injectors. Figure 12 shows a picture of the fuel injector array prior to installation in the combustion rig.

Installation of the test rig went relatively smoothly with completion of all installation tasks on Monday, August 27, 2012. Figure 13 is a picture of the installed combustor as seen from the rig's exhaust section looking upstream while Figure 14 is a picture from the side window of the rig showing the downstream face of the fuel injectors. Figure 15 is a picture of the injector assemblies taken upstream of the combustor.
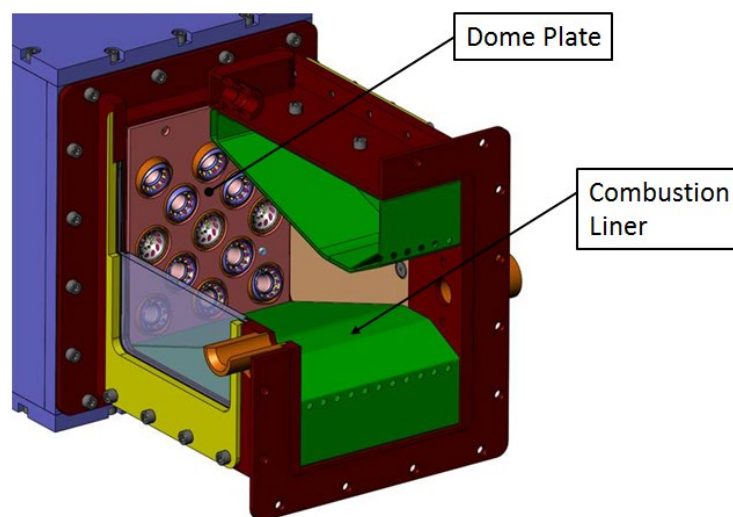

Figure 11.—Multi-Point Array with air blast fuel injectors installed in
the updated Medium Pressure Rig.

Figure 12.—Fuel injector assemblies for
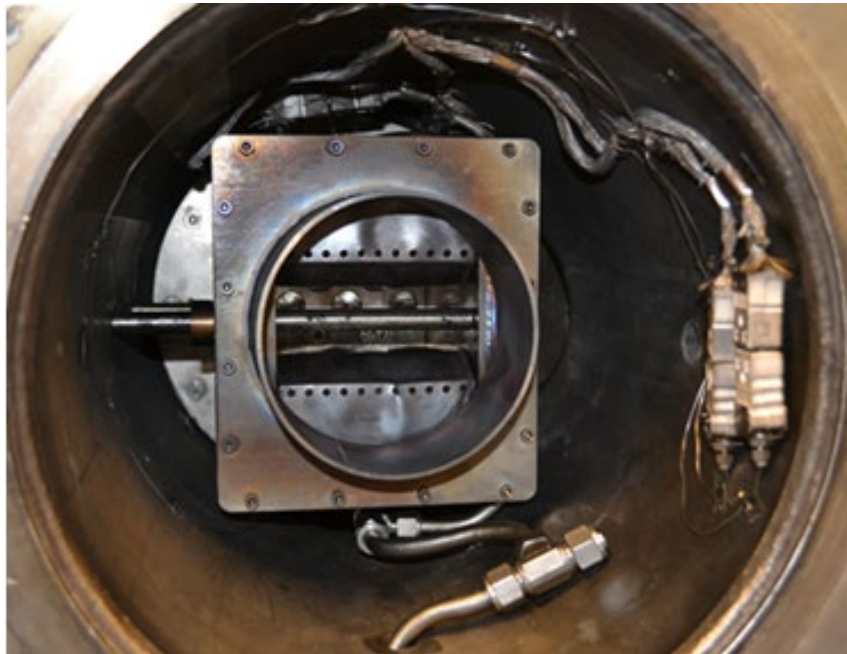Medium Pressure Rig testing at UC.

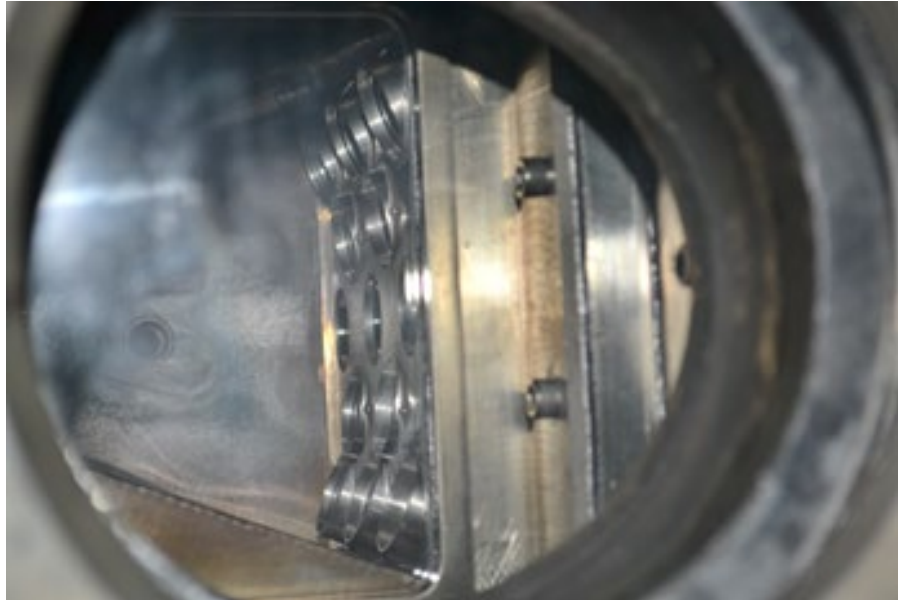Figure 13.—MLDI combustor installed in the Medium Pressure Rig at UC.

Figure 14.—MLDI combustor installed in the Medium Pressure Rig at UC.

Figure 15.—MLDI combustor installed in the Medium Pressure Rig at UC.

All testing planned for this week was completed within the allotted test window. This included testing with Jet-A and R-8 biofuel at idle conditions and conducting LBO tests. Most of the idle conditions tested used both the pilot and the intermediate fuel injectors with a few attempts at running idle conditions using all three fuel circuits. Some off idle testing was conducted, but only using the Jet-A fuel. Off idle testing did show some dynamic pressure oscillations as the pilot fuel was reduced without decreasing flow to the intermediate and the outer injectors. While dynamic pressure oscillations are a general concern for lean systems, they were easily controlled in this MLDI array by adjusting the fuel flow splits to avoid the problematic conditions. After completion of this round of testing, the equipment was left with the team at the UC in order to allow them to continue conducting tests on the rig and for them to have a system they could use to fine tune their new emissions test set-up. These tests may include using a different biofuel

and, possibly, using a different combustor liner which would change the combustion area. Because the rig was not dismantled, post-test pictures are not available.

Previous testing has shown marginally lower LBO when testing with R-8 as compared to Jet-A. Table 3 shows data from the latest testing which indicates a LBO for Jet A at an average FAR=0.0046 (ϕ=0.068) with a slightly reduced LBO for R-8 biofuel of FAR=0.0044 (ϕ=0.066). Tests 1, 2, 4, 5, and 6 were conducted starting from idle conditions of P3=55 psia, 4 percent ΔP, T3=434 °F using only the pilot fuel injectors. Test 3 was run at the same conditions except the ΔP was set at 2 percent.

Preliminary analysis of the emissions data from these tests indicated reasonable NOx values, slightly high unburnt hydrocarbons (UHC), and high levels of carbon monoxide (CO). Since this was the second combustion rig test using new emissions equipment, TFT is requesting that UC investigate the system further in order to fine tune the equipment. In addition, there is some concern that the cooled walls of the combustor may be causing higher than expected levels of UHC and CO. These cooled walls are not representative of an engine combustor wall.

During the month of September 2012, TFT shipped the CE-5 rig test design to NASA. A three-dimensional depiction of installation of the CE-5 rig design with the ceramic combustor is shown in Figure 16 and a picture of the final assembly is shown in Figure 17.

TABLE 3.—LBO DATA

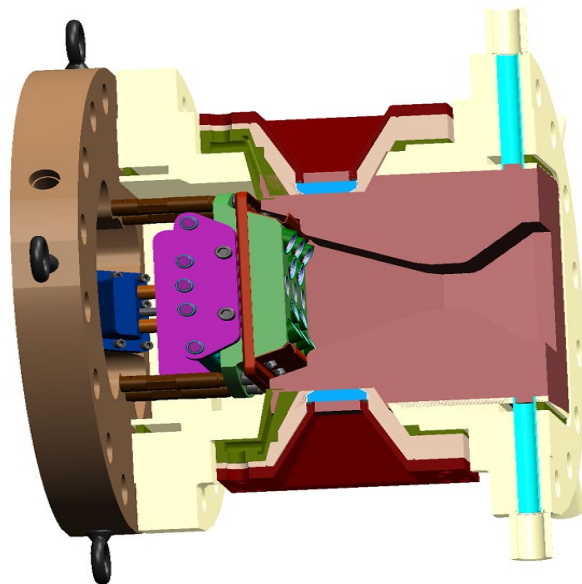| Test	Fuel	Fuel, lb/m	Air, lb/m	FAR	Equivalent ratio, ϕ	ACd, in^2
1	R-8	0.1812	41.537	0.00438	0.0642	1.747
2	R-8	0.1901	41.561	0.00457	0.0671	1.748
3	R-8	0.1296	30.220	0.00429	0.0629	1.798
4	Jet-A	0.2064	42.137	0.00490	0.0718	1.906
5	Jet-A	0.1855	42.061	0.00441	0.0647	1.936
6	Jet-A	0.1885	41.871	0.00450	0.0660	1.894

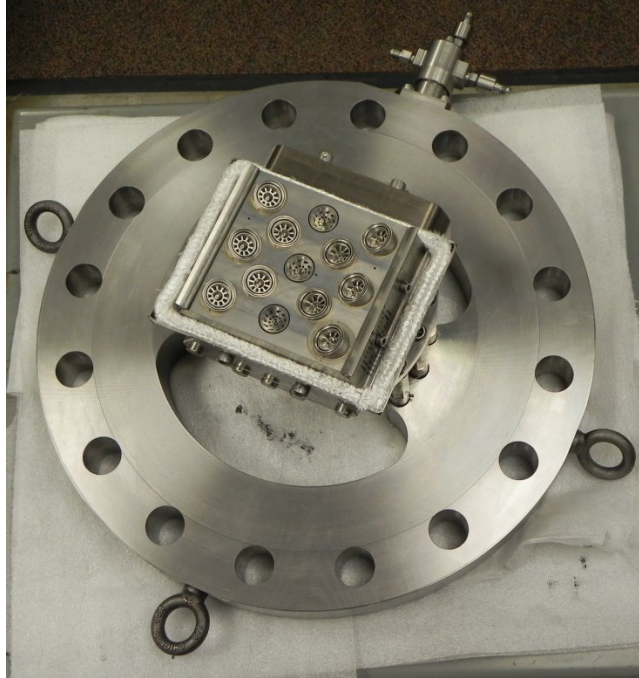Figure 16.—Integration of Goodrich MLDI in NASA CE-5 Rig.

Figure 17.—Final assembly of Goodrich MLDI for NASA CE-5 Rig.

Shortly after ignition, rig testing of this assembly was discontinued due to high temperatures (1700 °F) detected on the fuel manifolds upstream of the combustor. It was also noted just prior to shut down that the fuel flow was significantly higher than expected for flow through the pilot fuel circuit only. The assembly was then removed from the rig and inspected. Inspection showed damage to the lower section of the test assembly. Several injectors were damaged, and some were completely missing from the dome. Cause of this damage was most likely a fire upstream of the combustor as indicated by soot on the fuel manifolds.

The rig test assembly was then returned to TFT for evaluation. Fuel flow testing indicated slight leakage around the manifolds which were sealed using Kalrez o-rings, graphoil seals, and with ceramic epoxy around the heat shield. However, there was a significant leak detected at a bolted connection upstream of the o-ring locations. Further investigation indicated that the o-rings were completely eroded away in all but a few locations on the fuel manifolds. The resulting leakage allowed fuel into the air heat shield cavities, which then exited at the aforementioned bolt hole.

This fuel leak was caused by exposure of the o-rings to temperatures exceeding their 600 °F temperature capability. The o-rings were replaced on the rig components and retested. No overboard fuel leaks were detected with the new o-rings installed. In addition, the back-up graphoil seals (back up seal to the o-rings) did not provide sufficient sealing. It is important to note that the ceramic epoxy on the heat shields may have minimized the fuel leak and thus might have prevented a fire if the bolt on the flange had been sealed.

All analysis conducted prior to, and after, the o-ring failure indicates that the o-rings would have functioned as intended if fuel had been flowing through the pilot circuit during the temperature excursion to 1000 °F. In addition, this type of o-ring application is typical of fuel systems used in production aircraft engines. However, TFT understands the limitations and extreme conditions possible during rig testing and therefore decided to redesign the rig assembly to eliminate the o-rings in the fuel manifold to further reduce risk. Figure 18 is a three-dimensional depiction of the preliminary design of the new rig test assembly.
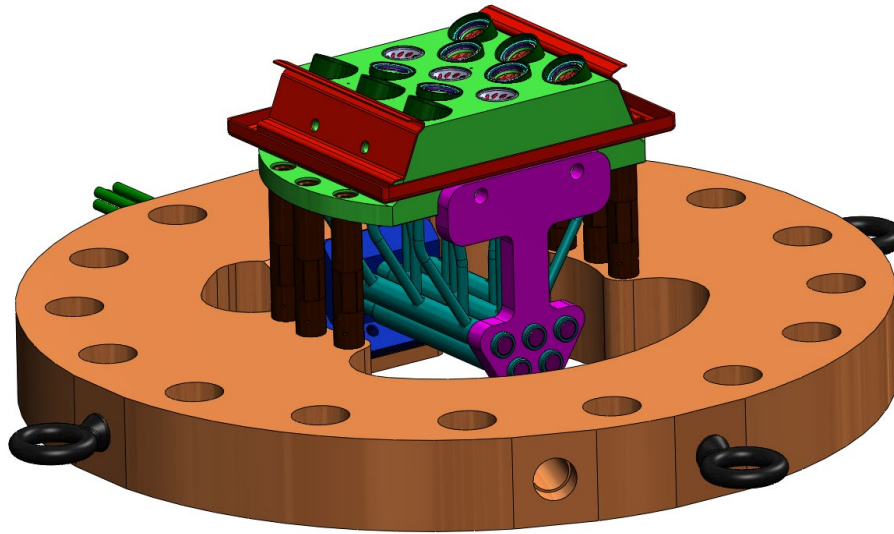
Figure 18.—Final Assembly Concept for Goodrich MLDI-NASA CE-5 Rig

TABLE 4.—GOODRICH MLDI PILOT LBO TEST DATA

Design	Test	Fuel, lb/m	Air, lb/m	FAR	Equivalent ratio, ϕ	ACd, in^2
Initial	1	0.2064	42.137	0.00490	0.0718	1.906
Initial	2	0.1855	42.061	0.00441	0.0647	1.936
Initial	3	0.1885	41.871	0.00450	0.0660	1.894
Revised	1	0.2453	40.081	0.00607	0.0886	2.017
Revised	2	0.2335	40.892	0.00571	0.0837	1.962
Revised	3	0.2305	40.316	0.00567	0.0831	2.008

Previous tests at the UC led to concerns regarding the levels of CO and UHC during idle. While TFT is not completely certain that these results are accurate, a review of the pilot design was completed in order to ascertain if the pilot's performance could be improved. TFT conducted tests of variations of pilot injector prototype designs in February 2013 and selected a new design based on improved performance at ambient conditions. The main parameters being measured at ambient temperature and pressure were light off and LBO. The new pilot design was then tested at the UC and the results were compared to the initial pilot design. Data from the testing at UC is shown in Table 4.

The results of these tests indicate the new pilot has not improved the LBO capability of the system. In addition, UHC and CO data between the two designs is very close to the same at idle conditions. Geometric changes to the pilot design are shown in Figure 19. Preliminary CFD analysis of the system with the new pilot indicates that the new design should not adversely impact the emissions of the system at full power as shown in Figure 20.
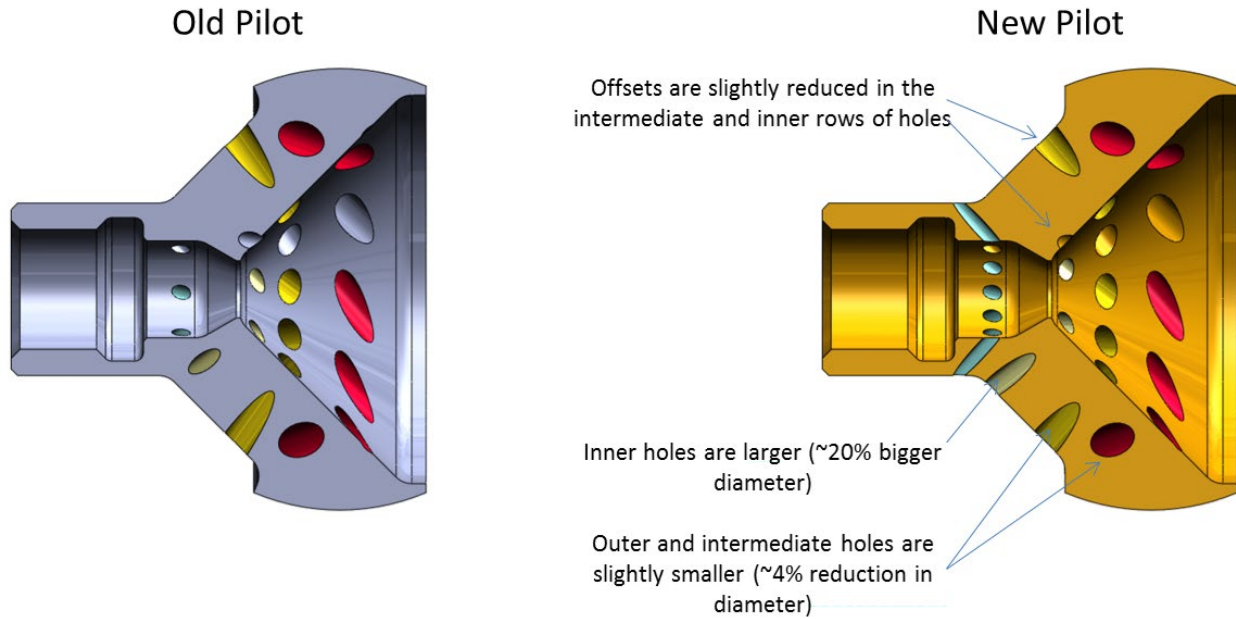
Old Pilot

New Pilot

Offsets are slightly reduced in the intermediate and inner rows of holes

Inner holes are larger (~20% bigger diameter)

Outer and intermediate holes are slightly smaller (~4% reduction in diameter)

Figure 19.—Revised Pilot Design for Goodrich MLDI-NASA CE-5 Rig.

New Pilot Design CFD
(diagonal slice through 5 nozzles)

Old Pilot Design CFD
(diagonal slice through 5 nozzles)
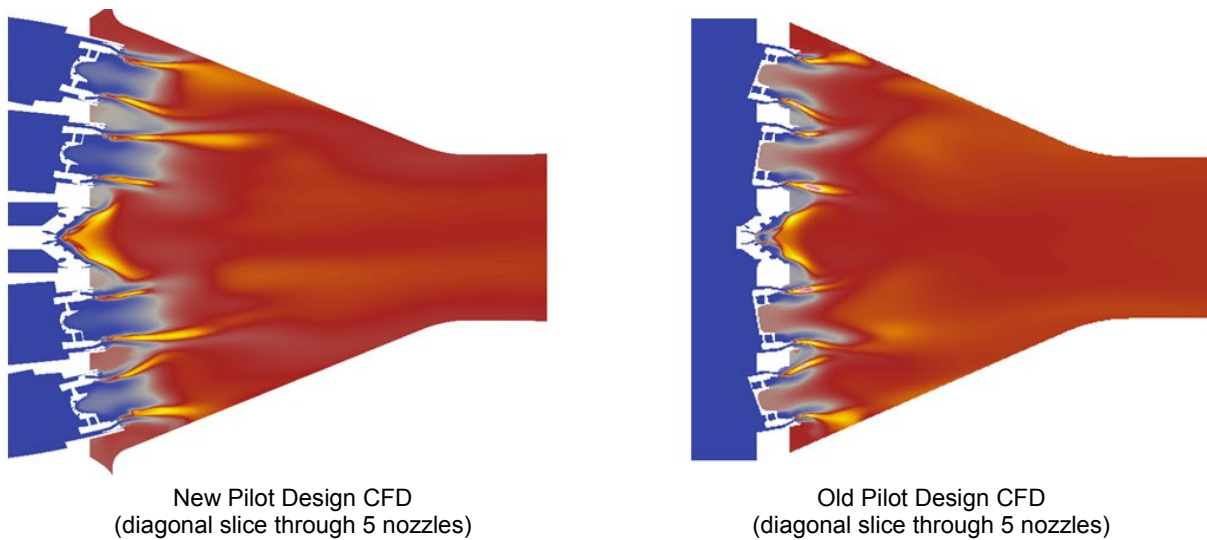
Figure 20.—CFD comparison between the New Pilot Design and the Old Pilot Design.

In preparation for testing in NASA's CE-5 combustion rig, TFT completed manufacture of spare assemblies for the rig test assembly in May of 2013. The additional assemblies, shown in Figure 21, were manufactured as a risk mitigation effort to ensure completion of the testing at NASA.

Additional high temperature, ambient pressure burn testing was completed on the intermediate and outer air blast fuel injectors as part of TFT's continued investigation into the operability of these designs. Figure 22 is a picture from one of these tests and Table 5 shows the data obtained during the testing.
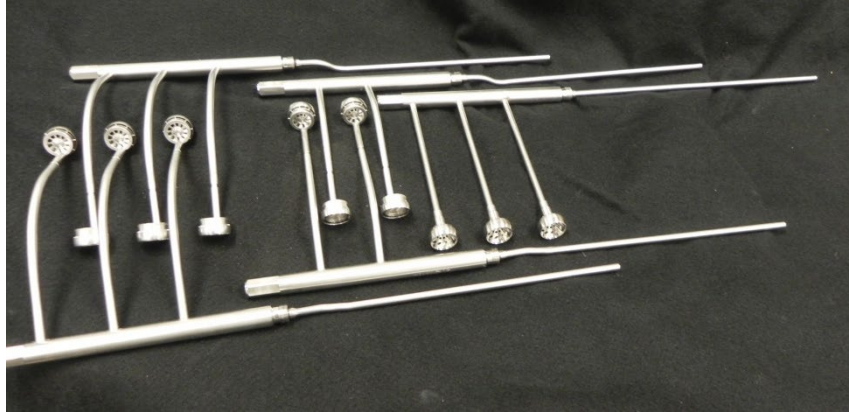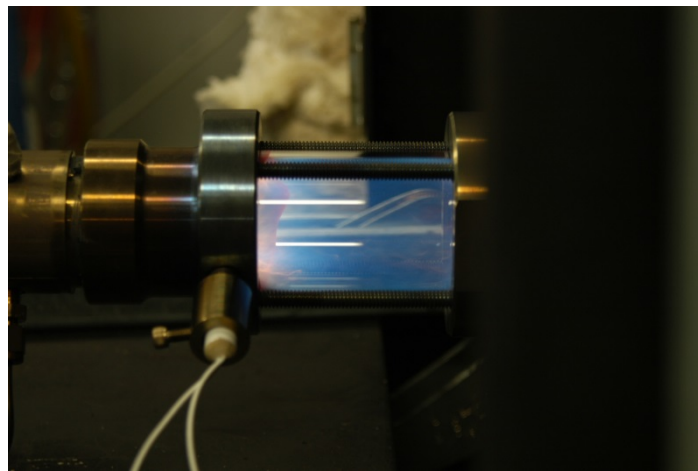
Figure 21.—Goodrich MLDI rig spare manifolds.

Figure 22.—Goodrich MLDI injector test at TFT.

TABLE 5.—GOODRICH MLDI INTERMEDIATE AND OUTER INJECTOR TEST DATA

Nozzle	Air pressure		Nozzle ACd, in^2	Air flow, lb/s	Fuel flow, pph	FAR	Equivalent ratio, ϕ
	in H$_2$O	psi					
1-in. intermediate	16	0.576	0.1877	0.0253	4.6	0.050505	0.742721
1-in. intermediate	16	0.576	0.1877	0.0253	3.5	0.038428	0.565114
1-in. intermediate	16	0.576	0.1877	0.0253	3	0.032938	0.484383
1-in. intermediate	16	0.576	0.1877	0.0253	2.6	0.028546	0.419799
1-in. intermediate	16	0.576	0.1877	0.0253	2.5	0.027448	0.403653
1-in. outer	16	0.576	0.1706	0.023	4	0.048309	0.710429
1-in. outer	16	0.576	0.1706	0.023	3.5	0.042271	0.621625
1-in. outer	16	0.576	0.1706	0.023	3	0.036232	0.532822
1-in. outer	16	0.576	0.1706	0.023	2.5	0.030193	0.444018
1-in. outer	16	0.576	0.1706	0.023	2	0.024155	0.355215
1-in. outer	16	0.576	0.1706	0.023	1.8	0.021739	0.319693
1-in. outer	16	0.576	0.1706	0.023	1.8	0.021739	0.319693

Medium pressure combustion rig testing at the UC was suspended in January due to heat damage to the combustion section of the rig. TFT then revised the design of the rig to improve its durability by changing the window design, increasing the size and number of screws on the window support, and implementing Greencast liners in place of metal liners. A picture of the new rig is shown in Figure 23.

Idle testing of the MLDI combustion system with the new pilot designs resulted in the data shown in Table 6. As indicated previously, the CO and UHC values are similar to those obtained with the previous design.

Figure 24 shows images of the chemiluminescence of the flame at various operating conditions. This analysis indicates a fairly well distributed flame when all three circuits are burning, which matches the visual appearance as shown in the photograph in Figure 25. All of these images were taken during testing at the UC.
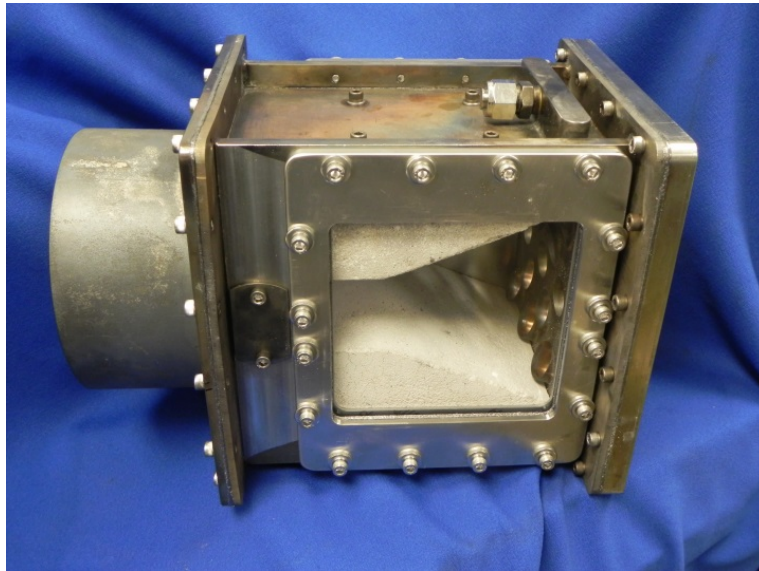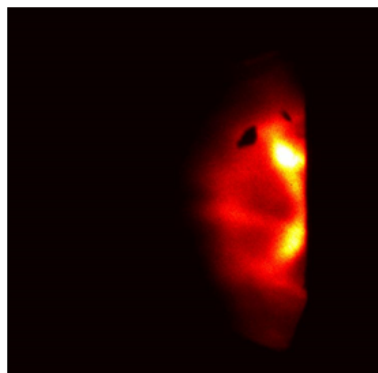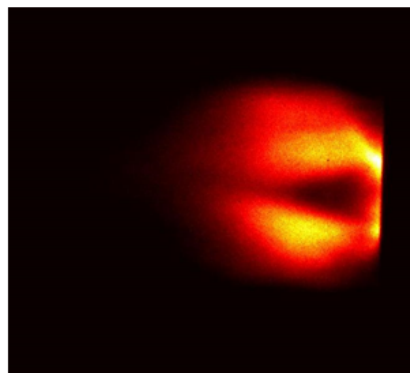

Figure 23.—Goodrich MLDI rig for testing at the UC.

TABLE 6.—GOODRICH MLDI TEST DATA

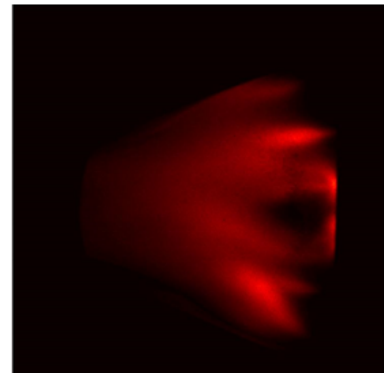|	Wf, lb/min			Emissions, ppm			Emissions, EI		
	Pilot	Intermediate	Outer	UHC	CO	NOx	UHC	CO	NOx
1	0.515	0.582	0	1643	1056	9.80	33.0	42.6	0.621
2	0.293	0.787	0	2343	1007	9.33	47.6	41.1	0.598

60 psi P4, 500 °F T3, 4 percent ΔP

Pilot only   Pilot + Intermediate 25% pilot, 75% inter   Pilot, Intermediate & Outer 12% P, 39% I, 49% O

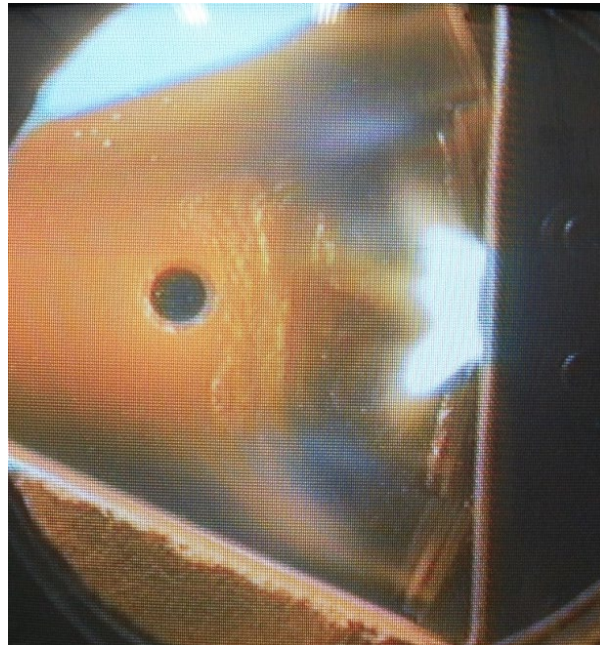Figure 24.—Chemiluminescence images taken at UC.

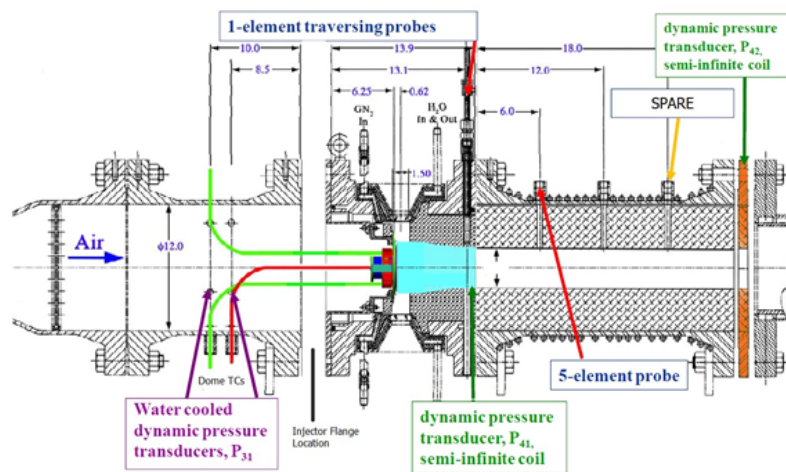Figure 25.—Picture of combustor with all fuel circuits burning.

Figure 26.—CE-5 schematic

This final design was tested in the NASA CE-5 rig (a rig schematic is shown in Figure 26) from May 28 to May 30, 2013. During this time, emissions test data was taken for conditions prescribed as NASA's design points, as well as other conditions that expanded the exploration of the design space or provided UTAS some benefit in evaluating their designs. This other data is tabulated at the end of this section; however, the majority of the report will focus on the design point data.

Prior to the test dates, two different sets of engine conditions were provided to UTAS from which to derive a test matrix. On arrival at NASA, it was explained that the evaluation of the different suppliers' designs would be made based on one of these two: a NASA/Pratt & Whitney cycle.

In building the new test matrix, UTAS maintained the FAR from the boundary conditions chart. However, most of the pressures and temperatures could not be attained on the CE-5 rig. Working with NASA, UTAS created the following table of modified test conditions that could be achieved. These were the test points for which data was obtained for comparison with the other companies, as shown in Table 7.

Testing at the design points involved running at all four conditions: idle, 30 percent power, cruise, and takeoff. For each of these conditions, UTAS varied fuel splits between its three independent circuits to find the lowest NOx emissions. The emissions data from these points are presented in this section as UTAS' results for evaluation on the ERA program.

Additionally, once a good fuel split was found for each condition, UTAS maintained those splits, but increased the overall fuel air ratio to observe the effect on emissions. This was intended to simulate the possibility of diverting a certain amount of air from the nozzles and adding it to the turbine cooling and leakage air (TCLA). In this way, UTAS would be able to see if diverting a portion of the air to TCLA would be beneficial to the system in future iterations. However, these points, by definition, did not meet the NASA design points.

Medium pressure testing at the UC showed that the idle condition was best reached using only the pilot injectors. Incorporating the intermediate circuit was possible, but it resulted in incomplete combustion and high levels of unburned hydrocarbons, due to the very lean local FAR at which the air blast injectors were operating. This was confirmed at NASA with one attempt at pilot-intermediate idle, after which all idle tests were done using only the pilot circuit. Testing at the design point then was limited to one condition, since there were no other circuits with which to split the fuel. Table 8 shows the results of the design point idle test, as well as conditions reflecting 10 and 15 percent bypass air to TCLA.

The trends of the emissions indices for these different fuel-to-air ratios are also shown visually in Figure 27 to Figure 29.

TABLE 7.—BOUNDARY CONDITIONS ADAPTED FOR CE-5 RIG

Condition	P3, psi	T3, °F	ΔP, %	FAR
Idle	77	500	3.30	0.0141
30% power	205	716	3.00	0.0214
Cruise	250	1000	3.50	0.0244
Takeoff	250	1030	4.00	0.0259

TABLE 8.—EMISSIONS INDICES FOR IDLE CONDITIONS
WITH 0, 10, AND 15 PERCENT TCLA

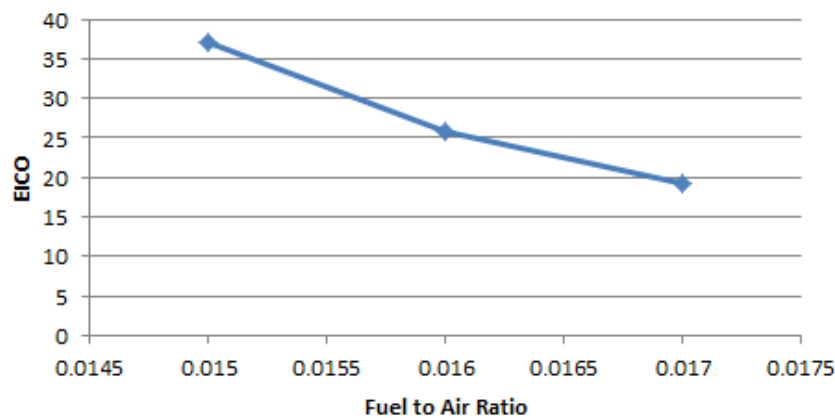| P3, psi	T3, °F	ΔP, %	FAR	Wf, p	EICO	EINOx	EIHC
72	502	3.65	0.015	56.7	37.18	4.6	2.7
81	508	3.27	0.016	66.2	25.7	4.9	1.69
82	509	3.31	0.017	71.1	19.21	5.0	1.54

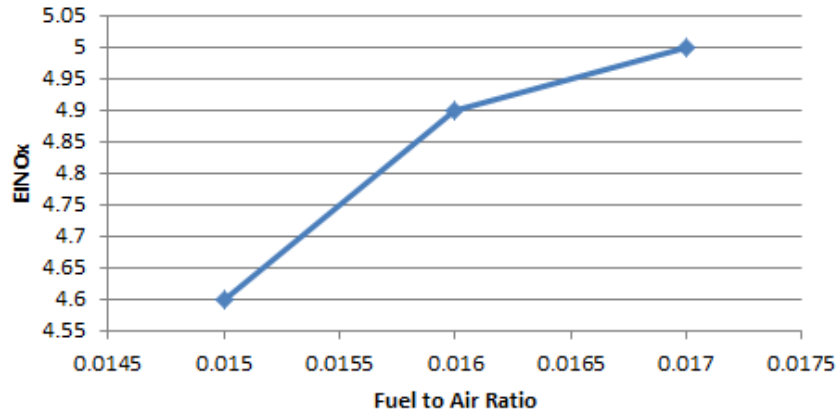Figure 27.—CO emissions at idle for varying fuel-to-air ratios.

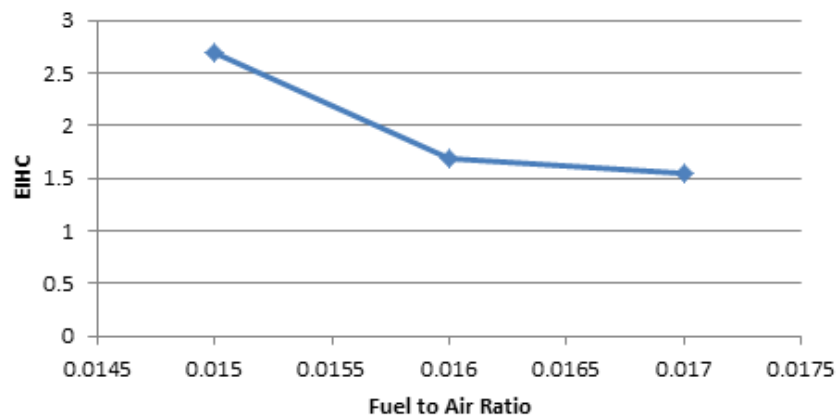Figure 28.—NOx emissions at idle for varying fuel-to-air ratios.

Figure 29.—UHC emissions at idle for varying fuel-to-air ratios.

Under the boundary conditions associated with this idle, NOx is not typically considered a concern. This is seen in UTAS testing with values below EINOx = 5 g-NOx/kg-fuel for all fuel-to-air ratios. UTAS's design was therefore intended to utilize the pilot injectors at low power to keep CO and UHC emissions low, with the staging of intermediate and outer injectors providing low NOx at higher power. Using the GE90 engine as an example for comparison, this result is achieved with very similar emissions at idle condition. The emissions comparison with this sample engine is shown in Table 9.

At 30 percent power, there were more options for how to set up the circuits. The design point fuel-to-air ratio made it possible to run with only the pilot and intermediate circuits, or with all circuits flowing. The data below is separated into these two different types of cases. For each, the overall fuel-to-air ratio was kept constant, but the splits between the circuits were varied. The emissions were recorded for each point. Table 10 shows the results for pilot and intermediate; Table 11 is similar for pilot, intermediate and outer. In each, the configuration with the lowest NOx is highlighted. Figure 30 to Figure 35 show the variation in emissions for the different splits.

The following three plots are for the pilot and intermediate nozzle condition. As shown in Table 10, the overall fuel-to-air ratio was kept constant, but the percentage of that fuel flow through each circuit was shifted. The plots give this independent variable as percent pilot. As the percentage of pilot flow increases, to maintain the same fuel-to-air ratio, there necessarily must be a corresponding decrease in intermediate flow rate.

As previously mentioned, the following tables and figures repeat the same procedure for the conditions where all three circuits are flowing fuel, as tabulated in Table 11. In these cases, the pilot percentage remained constant at about 26.9 percent of the fuel, while the percentage splits between intermediate and outer were varied. Again, the lowest NOx condition is highlighted.

TABLE 9.—IDLE COMPARISON BETWEEN UTAS AND GE90 ENGINE

Condition	EICO	EINOx	EIHC
GE90 idle	30.5	5.41	2.71
UTAS 0%	37.18	4.6	2.7
UTAS 10%	25.7	4.9	1.69
UTAS 15%	19.21	5.0	1.54

TABLE 10.—EMISSIONS AT 30 PERCENT POWER, DESIGN POINT,
PILOT AND INTERMEDIATE CIRCUITS ONLY

P3, psi	T3, °F	ΔP, %	FAR	Wf, p	Wf, i	EICO	EINOx	EIHC
206	729	2.96	0.02	70.7	116.4	3.85	10.81	0.63
202	730	3.06	0.021	52.4	142.7	1.89	9.82	0.33
206	725	3.01	0.021	25.9	168.5	7.44	8.7	0.33
207	723	3.05	0.022	21.8	181.2	3.31	9.97	0.31

TABLE 11.—EMISSIONS AT 30 PERCENT POWER, DESIGN POINT, ALL CIRCUITS

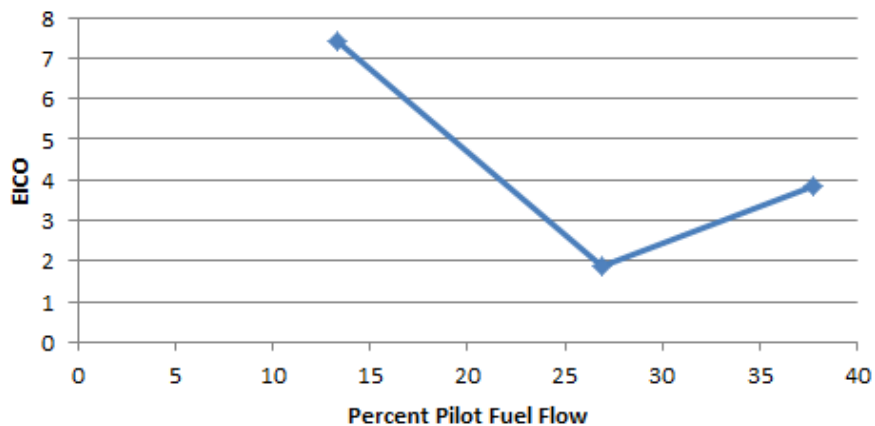| P3, psi	T3, °F	ΔP, %	FAR	Wf, p	Wf, i	Wf, o	EICO	EINOx	EIHC
199	718	3.04	0.02	63.5	44.1	75.8	83.48	3.56	0
201	718	3	0.021	52.1	54.1	87.2	18.26	2.3	0.03
199	718	3.04	0.021	52.1	62.2	79.3	11.37	2.45	0.02
201	717	3	0.021	52	71.9	69	10.11	2.77	0.01
197	718	3.19	0.021	51.5	72.1	69.1	13.04	2.38	0.21
200	718	3.1	0.021	31	83.3	80.3	16.79	1.23	0.1

Figure 30.—CO emissions at 30 percent power design point for varying fuel splits, pilot/intermediate circuits.
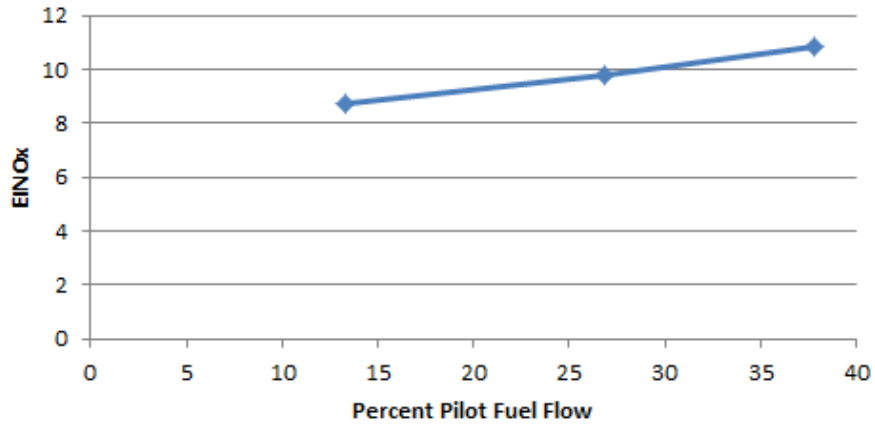
Figure 31.—NOx emissions at 30 percent power design point for varying fuel splits, pilot/intermediate circuits.
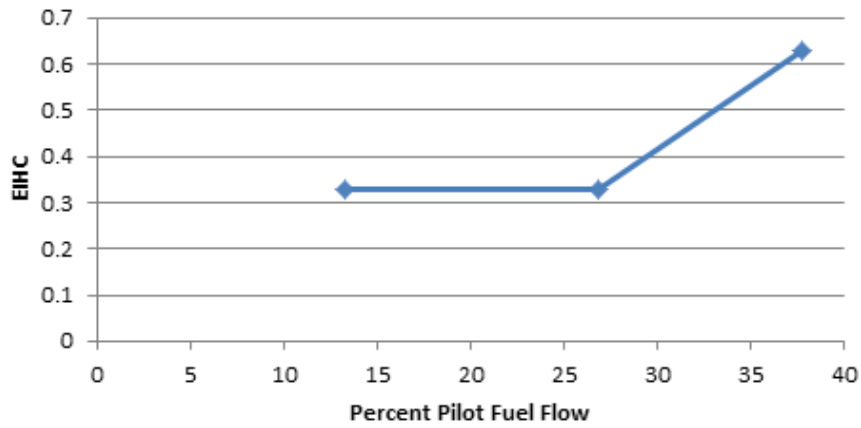

Figure 32.—UHC emissions at 30 percent power design point for varying fuel splits, pilot/intermediate circuits.
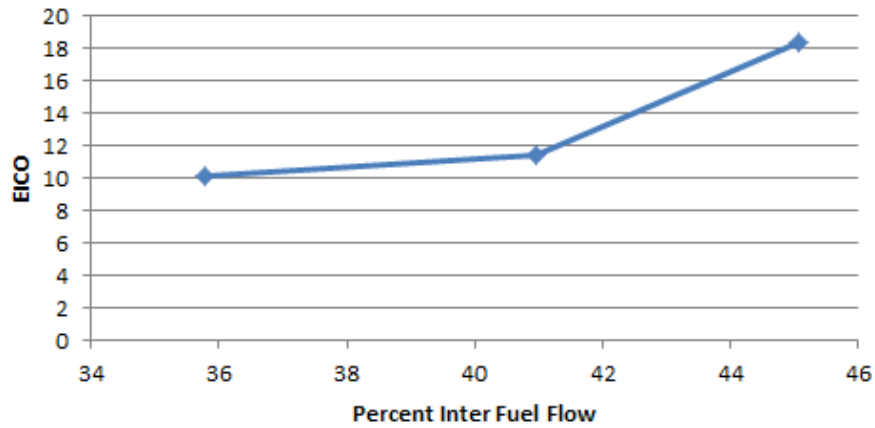

Figure 33.—CO emissions at 30 percent power design point for varying fuel splits, pilot/intermediate/outer circuits.
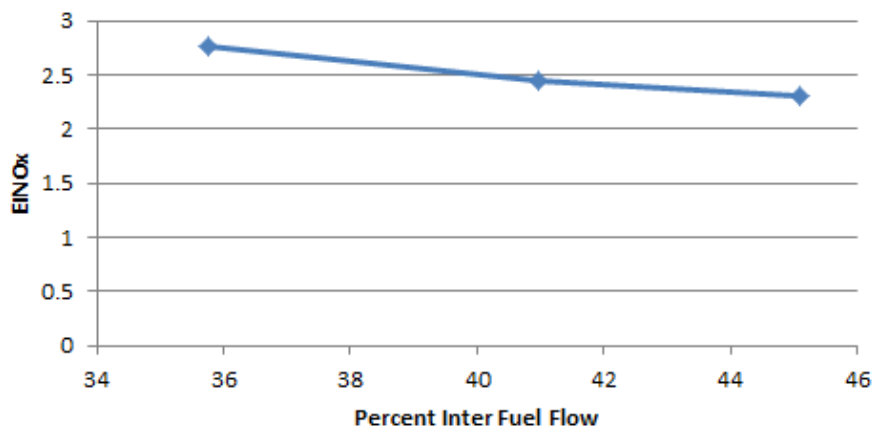
Figure 34.—NOx emissions at 30 percent power design point for varying fuel splits, pilot/intermediate/outer circuits.
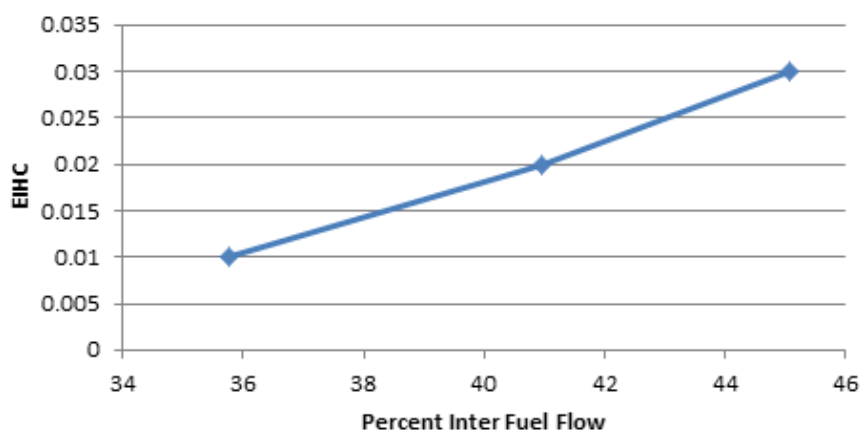

Figure 35.—UHC emissions at 30 percent power design point for varying fuel splits, pilot/intermediate/outer circuits.

TABLE 12.—COMPARISON OF TCLA AMOUNTS AT 30 PERCENT POWER WITH PILOT/INTERMEDIATE CIRCUITS

TCLA, %	P3, psi	T3, °F	ΔP, %	FAR	Wf, p	Wf, i	EICO	EINOx	EIHC
0	202	730	3.06	0.02	52.4	143	1.89	9.82	0.33
10	207	721	3.00	0.02	60.7	163	0.32	12.21	0.26
15	210	720	2.80	0.03	62.8	170	0.2	13.1	0.21

TABLE 13.—COMPARISON OF TCLA AMOUNTS AT 30 PERCENT POWER WITH ALL CIRCUITS

TCLA, %	P3, psi	T3, °F	ΔP, %	FAR	Wf, p	Wf, i	Wf, i	EICO	EINOx	EIHC
0	201	717	3.00	0.02	52	71.9	69	10.11	2.77	0.01
10	204	719	2.90	0.02	60.1	82.9	80	0.54	3.82	0.05
15	204	719	2.96	0.03	61.8	87.2	83.3	0.13	4.52	0.03

For both types of 30 percent power conditions, one test point was selected for variation of fuel air ratio. This was to evaluate the effect of bypassing the dome with a portion of the air and adding it to TCLA. Initially, selection of this point was intended to be based on NOx emissions alone. However, CO emissions were also highly variable at 30 percent power, so for these instances, a compromise condition was chosen with moderate levels of both emissions. The results of these comparisons are shown in Table 12 and Table 13, and also visually in Figure 36 to Figure 38.
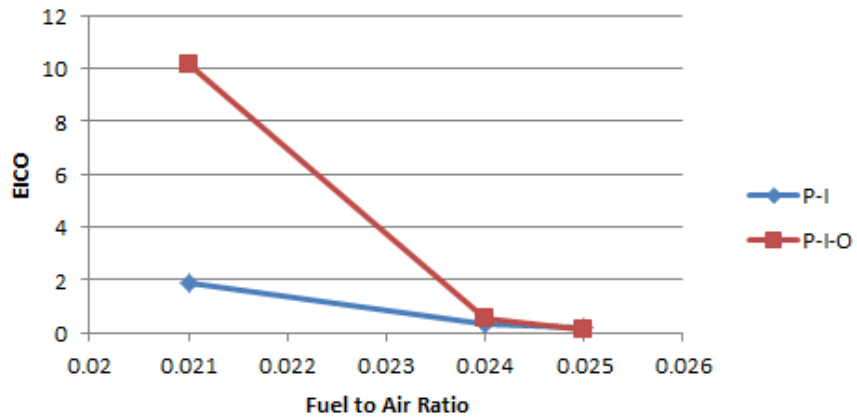
Figure 36.—CO emissions at 30 percent power for varying fuel-to-air ratios.
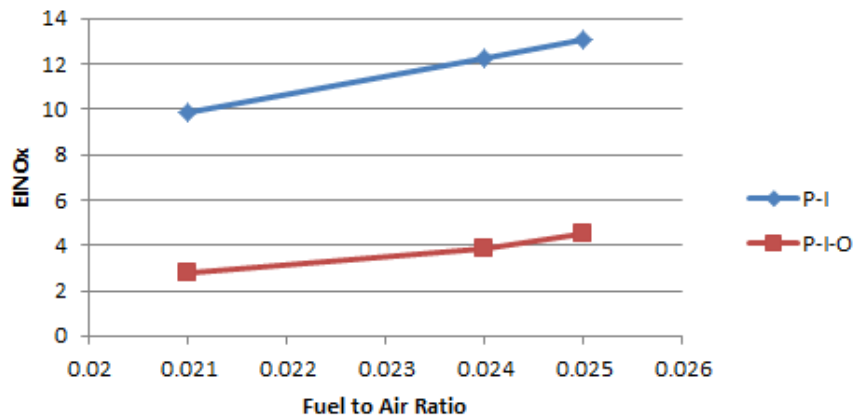

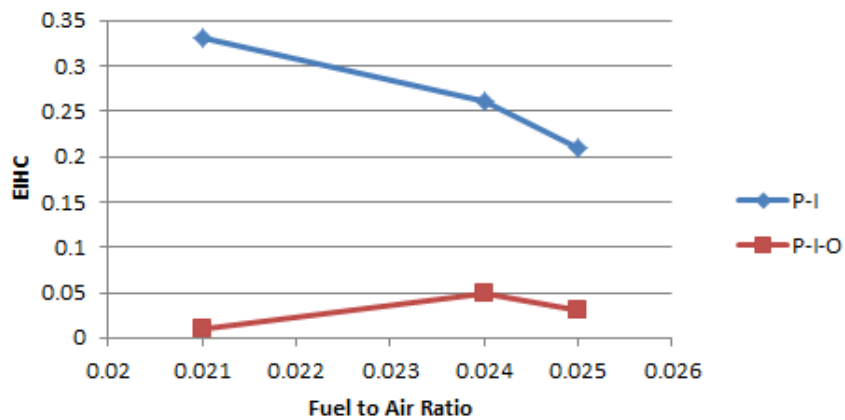Figure 37.—NOx emissions at 30 percent power for varying fuel-to-air ratios.

Figure 38.—UHC emissions at 30 percent power for varying fuel-to-air ratios.

Shown here, there is a clear tradeoff between the two types of 30 percent power conditions. Running at 30 percent with only pilot and intermediate nozzles shows a noticeable shift toward higher NOx and UHC emissions. However, that is offset by the lower CO emissions, particularly at the design point. Interestingly, although adding bypass air to TCLA has a minor effect on NOx and UHC, it significantly decreases CO emissions when all circuits are flowing. If running any bypass air, CO emissions are arguably identical for either type of 30 percent power case. Further study would be beneficial at this power condition to determine how stark this tradeoff is, or whether there is some split that maintains low CO, NOx and UHCs.

Note that many of UTAS' attempted fuel splits at 30 percent power were simply unattainable. In some instances this was due to elevated dome temperatures, which was not designed to exceed 1900 °F. In other cases, NASA fuel valve setup limited the range of the splits. At these times, one fuel circuit's valve would be fully opened and another nearly fully shut but not reaching the desired split. The pressure in the line feeding both valves could be increased or decreased, but there was no way to increase the difference in fuel flow. Alternate valve setup may have allowed for greater variety of test runs at 30 percent power, which may have further improved emissions.

Increasing power to the cruise condition brought the temperature and pressure up, and increased the number of variables that could be changed. Whereas 30 percent power tests were restricted by valve limitations and dome temperature concerns to just a few different pilot fuel flows, the cruise condition was able to run at a much wider range of fuel splits. For all of these cases, the pilot, intermediate, and outer lines were flowing fuel. At the design point fuel air ratio, a percent split through the pilot was chosen, and the percent through the intermediate and outer lines was varied. Then the percent through the pilot was changed and the process repeated to obtain a series of trends for emissions at differing splits. The data for these tests is given in Table 14, with the lowest NOx condition highlighted.

TABLE 14.—EMISSIONS AT CRUISE, DESIGN POINT, ALL CIRCUITS

P3, psi	T3, °F	ΔP, %	FAR	Wf, p	Wf, i	Wf, o	EICO	EINOx	EIHC
251	1007	3.43	0.024	35.4	87.2	139.1	0.01	3.18	0.05
249	1009	3.5	0.024	35.4	99.5	127.4	0.01	3.09	0.01
250	1008	3.57	0.024	35.4	115.5	111.4	0	4.3	0.01
251	1010	3.5	0.024	31.9	88.1	141.1	0.04	3.09	0
251	1010	3.46	0.024	31.8	101	129	0.01	3.02	0
251	1009	3.47	0.024	31.7	117	112.1	0.02	4.66	0.06
250	1010	3.43	0.024	27.9	89.9	144.6	0.01	3.71	0.01
251	1009	3.39	0.024	28	102.4	131	0.02	3.44	0
250	1008	3.52	0.024	28	119.2	114.2	0	4.5	0
251	1007	3.37	0.024	24.1	90.9	146.4	0.01	3.56	0
251	1007	3.36	0.024	24.1	104.4	133	0	3.58	0
252	1006	3.37	0.025	24.1	121	115.8	0.01	4.54	0
250	1006	3.39	0.024	21	92	148.8	0.01	3.81	0
249	1006	3.42	0.025	21	105.6	135.7	0.03	3.67	0
250	1005	3.33	0.025	21	123.4	118.3	0.01	4.62	0.02
249	1005	3.36	0.025	17.2	93.8	149.6	0.01	4.03	0.01
249	1006	3.39	0.025	17.3	107.1	136.8	0.02	3.78	0
248	1007	3.44	0.025	17.2	124.2	118.9	0.01	4.61	0
249	1006	3.4	0.025	34.8	111.6	114.4	0.01	4.78	0

These trends are perhaps better shown visually, as in the following three figures. First, CO emissions are shown, although these are quite low overall and do not provide much insight as to the best split. Figure 40 is the same type of plot for NOx, which is much more of the driving emission index at cruise. In both plots, individual lines are charted for each percent pilot series that was tested. These lines plot the emissions index on the vertical axis versus the percent fuel flow split through the intermediate circuit. In this way, both variables can be studied for their effect on emissions. This is shown in Figure 39 and Figure 40. Note that no plot is given for unburned hydrocarbons, because at these conditions their contribution is negligible.

Another way to view the dependence of NOx emissions on two independent variables is shown in a three-dimensional plot in Figure 41. In this chart, the surface represents emissions index of NOx, while the two independent axes are percent pilot and percent intermediate. The lowest valleys of the surface represent the lowest NOx, which can then be correlated to the flow splits that generated them.

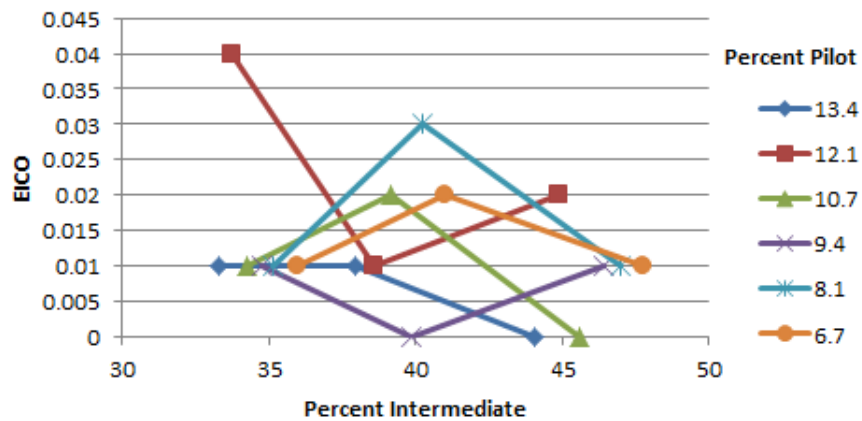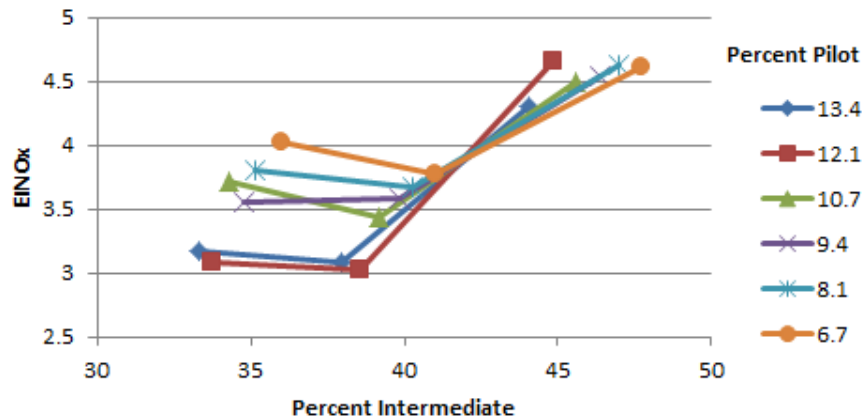Figure 39.—CO emissions at cruise design point for varying fuel splits.

Figure 40.—NOx emissions at cruise design point for varying fuel splits.

Clearly, the lowest NOx levels occur when the percent pilot is at its highest local fuel air ratio (although still much leaner than the air blast injectors), and the percent intermediate is at its lowest fuel air ratio. This matches the values shown in Table 15, where minimum NOx was achieved with flows of 31.8, 101, and 129 pph through the pilot, intermediate and outer lines, respectively. This gave a minimum EINOx value of 3.02.

From the best result, once again the fuel air ratio was varied so UTAS could study the effect of allowing some air to bypass the injectors and be added to cooling air. The data for these tests are shown in Table 16 and the corresponding plots in Figure 42 and Figure 43. Once again, unburned hydrocarbons were consistently low as expected and are not plotted here.
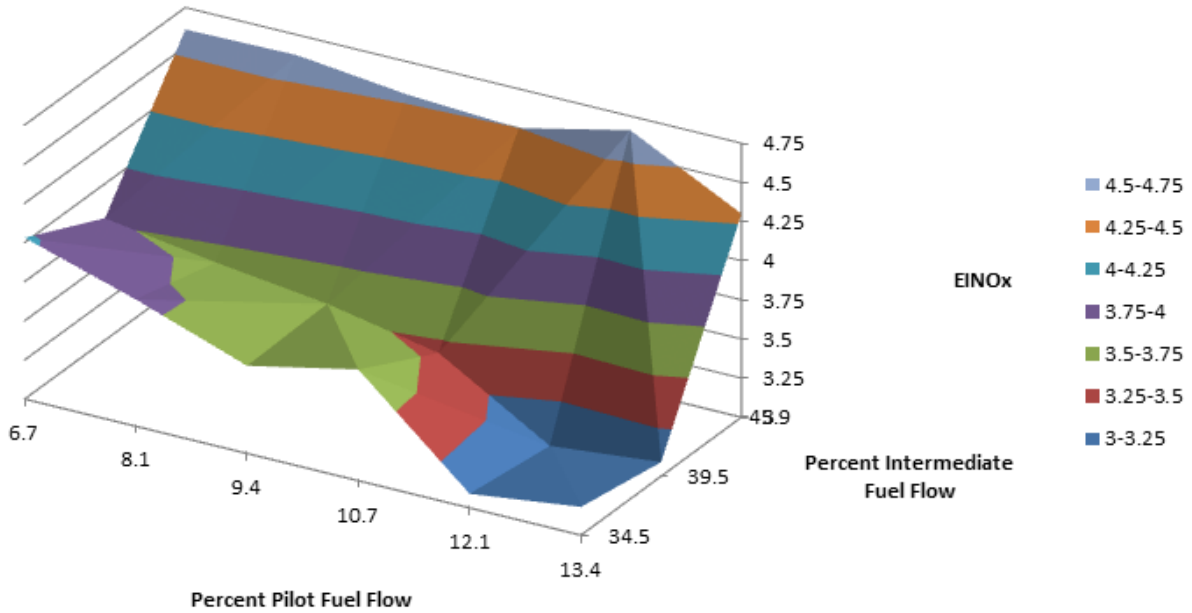

Figure 41.—NOx emissions at cruise design point for varying fuel splits

TABLE 15.—COMPARISON OF TCLA AMOUNTS AT CRUISE

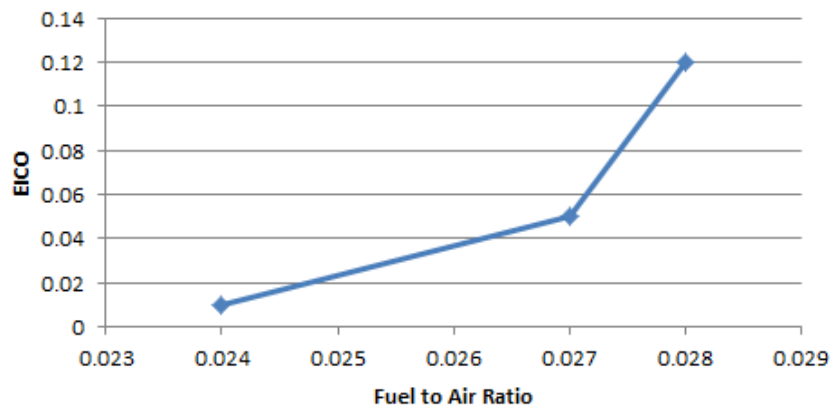| TCLA, %	P3, psi	T3, °F	ΔP, %	FAR	Wf, p	Wf, i	Wf, o	EICO	EINOx	EIHC
0	251	1007	3.37	0.024	24.1	90.9	146.4	0.01	3.56	0
10	251	1011	3.6	0.027	28	103	164.2	0.05	5.7	0
15	251	1009	3.68	0.028	29	107.1	170.7	0.12	7.68	0

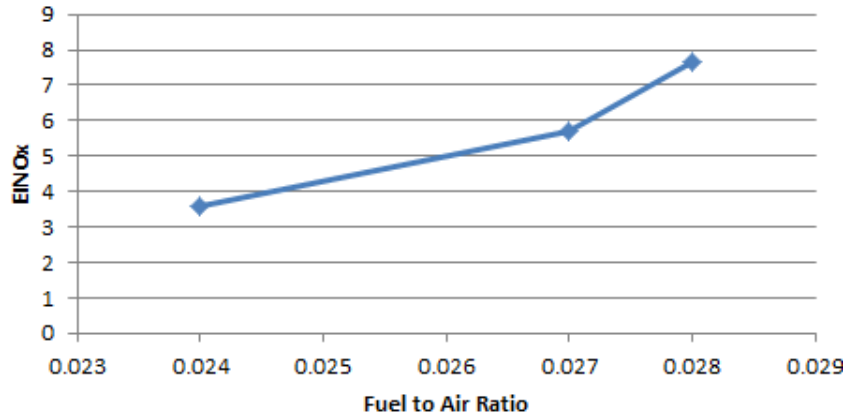Figure 42.—CO emissions at cruise for varying fuel-to-air ratios.

Figure 43.—NOx emissions at cruise for varying fuel-to-air ratios.

TABLE 16.—EMISSIONS AT TAKEOFF, DESIGN POINT, ALL CIRCUITS

P3, psi	T3, °F	ΔP, %	FAR	Wf, p	Wf, i	Wf, o	EICO	EINOx	EIHC
249	1033	4.17	0.026	35.4	100.7	161.8	0.33	4.53	0.11
248	1032	4.27	0.025	36	115.1	147.8	0.03	4.33	0
249	1031	4.29	0.025	35.9	133.8	128.6	0.02	5.2	0
249	1030	4.27	0.025	32.3	102.3	163.8	0.03	4.47	0
247	1030	4.34	0.025	31.9	117.2	150	0.03	4.06	0
248	1029	4.22	0.025	31.9	136.2	131.1	0.02	5.17	0
247	1028	4.35	0.025	28	104.1	167	0.02	4.39	0
247	1029	4.34	0.025	27.7	119	151.3	0.03	4.24	0
248	1028	4.31	0.025	27.9	137.9	132.9	0.01	5.05	0
248	1028	4.26	0.025	23.8	105.8	169.11	0.03	4	0
249	1029	4.26	0.025	24	121.1	153.5	0.05	3.98	0
249	1028	4.14	0.025	24	140	135.1	0.02	4.96	0
248	1028	4.34	0.025	20.9	106.7	172.1	0.03	4.17	0
249	1029	4.17	0.026	20.9	122.4	156.8	0.02	4.16	0
249	1028	4.21	0.026	20.8	142.1	136.8	0.02	4.85	0

For both measured emissions indices, the amount of the pollutant increases with increased fuel air ratio, indicating that at cruise, the concept of adding bypass air to cooling does not benefit the design.

Takeoff testing was performed very similarly to cruise testing. The T3 temperature increased from 1000 to 1030 °F, and the fuel air ratio increased from FAR=0.0244 to 0.0259. However, the test process followed the same steps as listed for cruise: changing pilot, intermediate and outer flow splits to find the lowest NOx emissions, then vary overall fuel air ratio for bypass air considerations. The data is shown in the same manner as for cruise. Data is shown in Table 16, followed by individual line plots in Figure 44 and Figure 45. Figure 46 is a three-dimensional representation of the design space, looking for a minimum EINOx level.
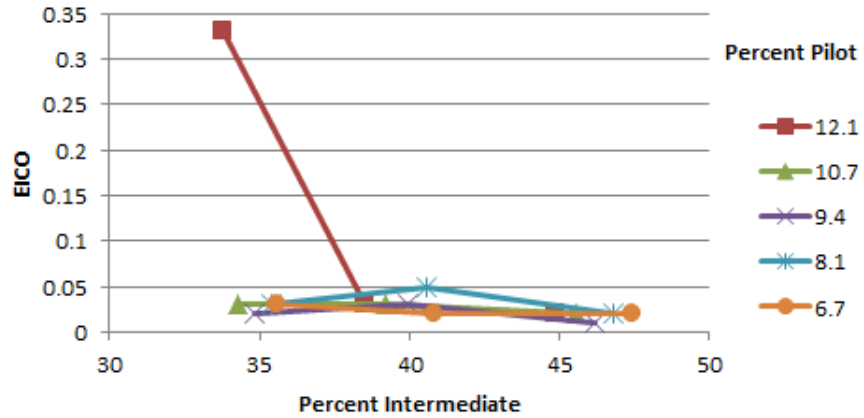
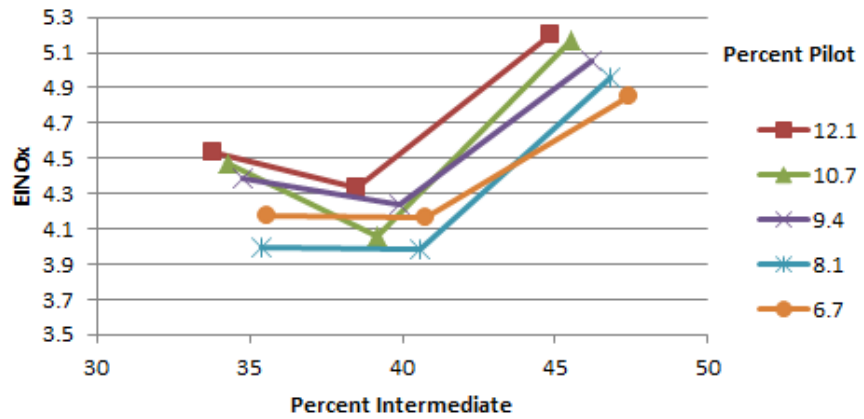Figure 44.—CO emissions at takeoff design point for varying fuel splits

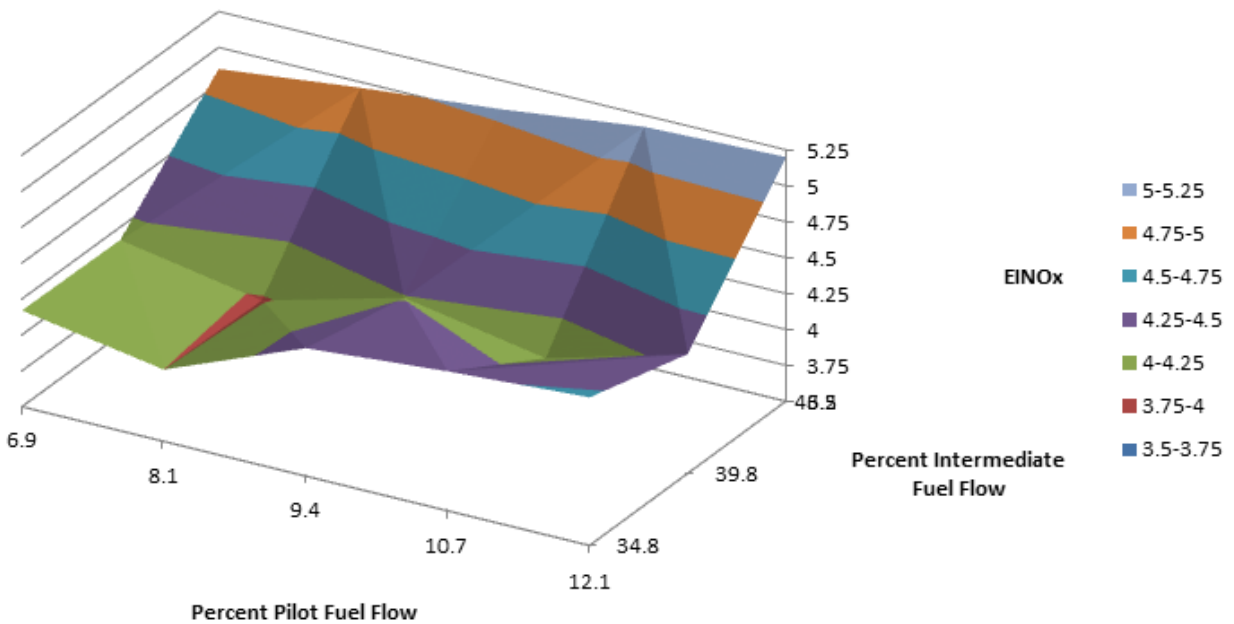Figure 45.—NOx emissions at takeoff design point for varying fuel splits

Figure 46.—NOx emissions at takeoff design point for varying fuel splits

Here again the minimum NOx level occurs with a lower percent flow through the intermediate circuit, meaning more flow through the outer nozzles. This trend also occurred at cruise. However, unlike cruise, NOx is lower at a somewhat lower percentage of pilot flow. The minimum of 3.98 EINOx occurs with 24, 121.1, and 153.5 pph of fuel flow through the pilot, intermediate and outer circuits, respectively. The minimum NOx found within the design space for this test condition was not limited by high dome temperatures or the fuel control valve configuration.

As was done with the prior test conditions, once an acceptable emissions level was found, the fuel air ratio was varied to see the effect more air to TCLA would have on the system. Table 17 shows this information in a tabular fashion, while Figure 47 and Figure 48 plot CO and NOx. Unburned hydrocarbons are ignored due to their lack of measurable amounts throughout.

TABLE 17.—COMPARISON OF TCLA AMOUNTS AT TAKEOFF

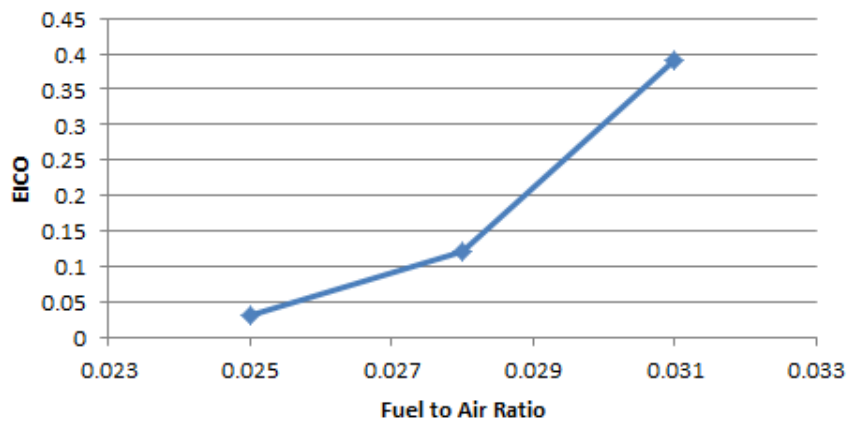| TCLA, %	P3, psi	T3, °F	ΔP, %	FAR	Wf, p	Wf, i	Wf, o	EICO	EINOx	EIHC
0	248	1028	4.26	0.025	23.8	105.8	169.1	0.03	4	0
10	251	1029	4.12	0.028	26	114	183	0.12	7.15	0
15	254	1028	3.62	0.031	28	121.4	196.2	0.39	12.09	0

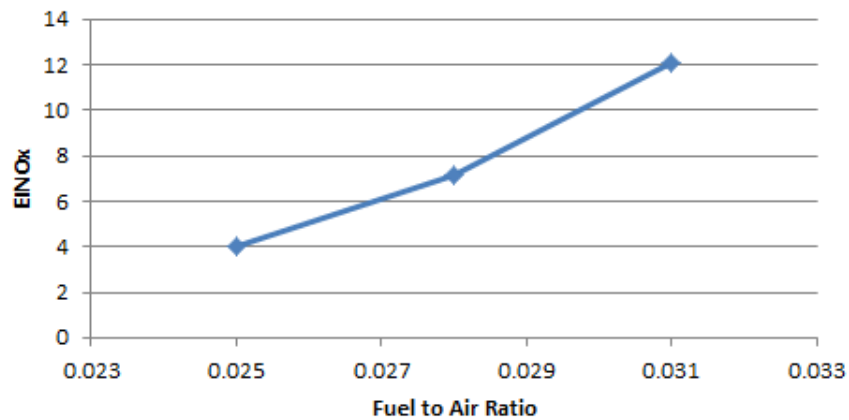Figure 47.—CO emissions at takeoff for varying fuel-to-air ratios.

Figure 48.—NOx emissions at takeoff for varying fuel-to-air ratios.

The results of the fuel air variation mimic those seen at cruise, where the emissions indices increase as the fuel air ratio rises. This is not entirely unexpected, and could be acceptable, provided the increased fuel air ratio provides benefits in emissions for low power cases.

With each condition tested at various fuel splits, the entire cycle of test points was tabulated and plotted. At each condition prescribed by NASA in the given boundary conditions, the split with the lowest NOx emissions was selected. All emissions indices are listed and plotted, corresponding to UTAS' best fuel splits at the mandated fuel-to-air ratio. At 30 percent power, the better NOx result was achieved with all three circuits flowing fuel, rather than just the pilot and intermediate, so that case is listed here. Overall, EINOx ranges from 1.23 to 4.60 g-NOx/kg-fuel while CO and UHCs are maintained at levels similar to current aircraft engines as shown in Table 18 and graphed in Figure 49 to Figure 51.

TABLE 18.—LOWEST-NOX EMISSIONS INDEX FOR EACH CYCLE POINT

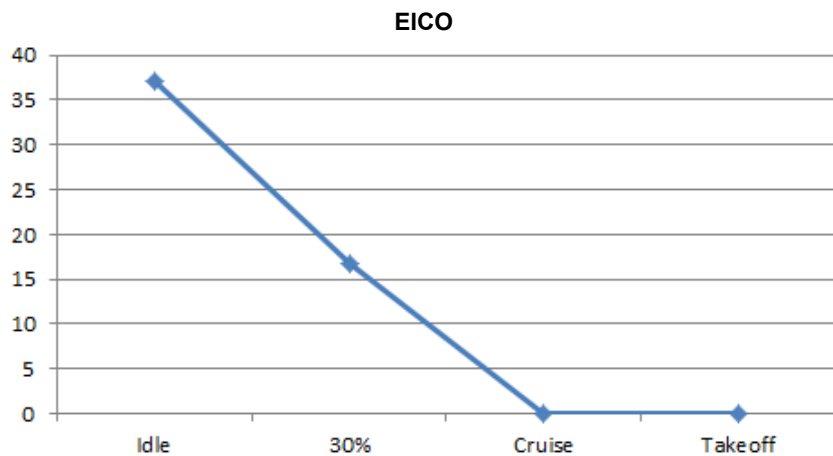| Condition	P3, psi	T3, °F	ΔP, %	FAR	Wf, p	Wf, i	Wf, o	EICO	EINOx	EIHC
Idle	72	502	3.65	0.015	56.7	0	0	37.18	4.6	2.7
30%	200	718	3.1	0.021	31	83.3	80.3	16.79	1.23	0.1
Cruise	251	1010	3.46	0.024	31.8	101	129	0.01	3.02	0
Takeoff	249	1029	4.26	0.025	24	121.1	153.5	0.05	3.98	0

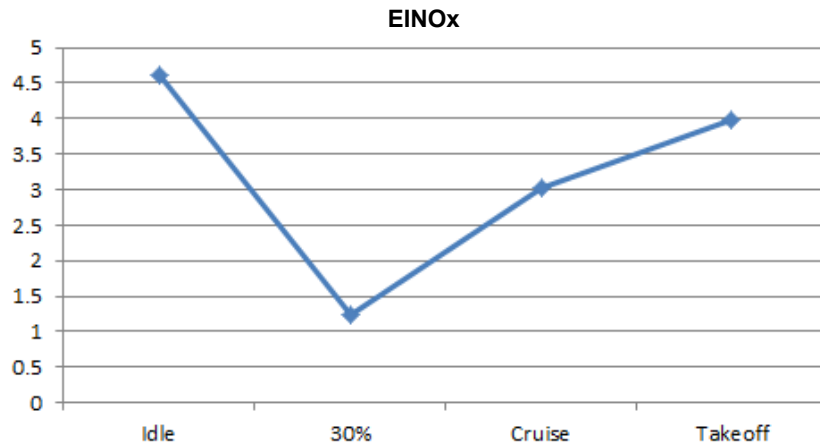Figure 49.—Lowest-NOx condition—CO emissions for full cycle.

Figure 50.—Lowest-NOx condition—NOx emissions for full cycle.

To further explore the design space, UTAS plotted the same cycle, but overlaid with the TCLA variation cases that were run. Here, the percentage splits through the different circuits were maintained, but the fuel-to-air ratio varied. Emissions are plotted in Figure 52 to Figure 54, while the numerical data that generated these plots is given in Table 19. Note that the 0 percent TCLA case does not necessarily correspond to UTAS' lowest NOx cases above. In some cases the lowest NOx fuel splits were not achievable, or simply not selected to run, at higher FAR. This data shows the trend of increased bypass air to TCLA but is not necessarily the "best" result.
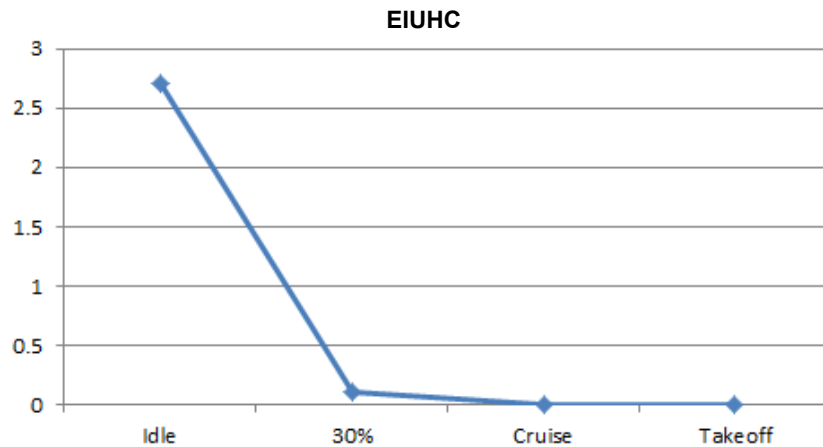

Figure 51.—Lowest-NOx condition—UHC emissions for full cycle.

TABLE 19.—EMISSIONS INDICES FOR FULL CYCLE AT VARYING LEVELS OF TCLA

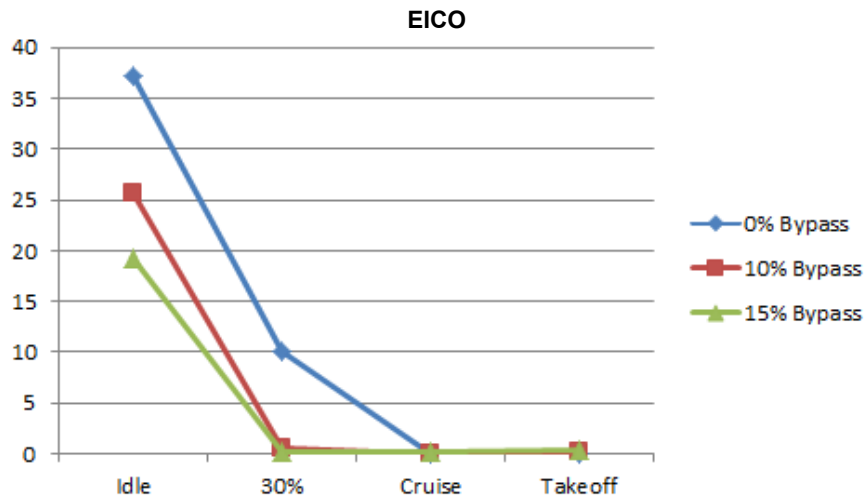| TCLA, %	EICO				EINOx				EIHC			
	Idle	30%	Cruise	Takeoff	Idle	30%	Cruise	Takeoff	Idle	30%	Cruise	Takeoff
0	37.18	10.11	0.01	0.03	4.6	2.77	3.56	4	2.7	0.01	0	0
10	25.7	0.54	0.05	0.12	4.9	3.82	5.7	7.15	1.69	0.05	0	0
15	19.21	0.13	0.12	0.39	5	4.52	7.68	12.09	1.54	0.03	0	0

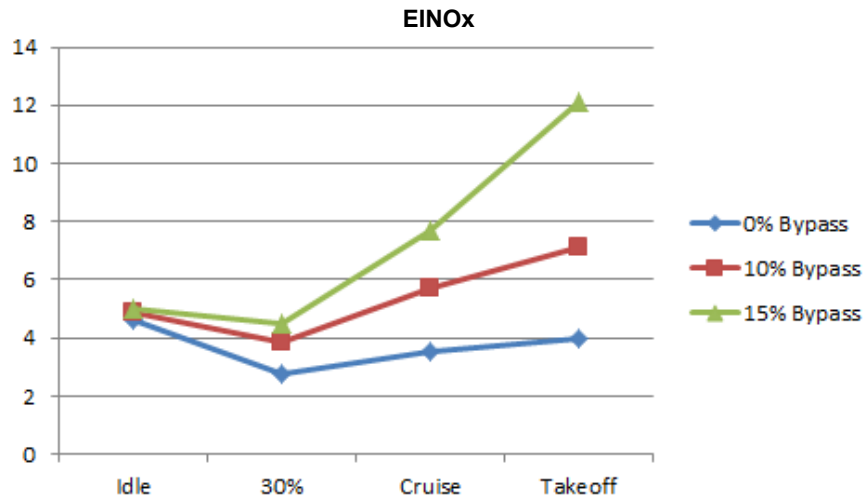Figure 52.—CO emissions for full cycle at varying levels of TCLA.

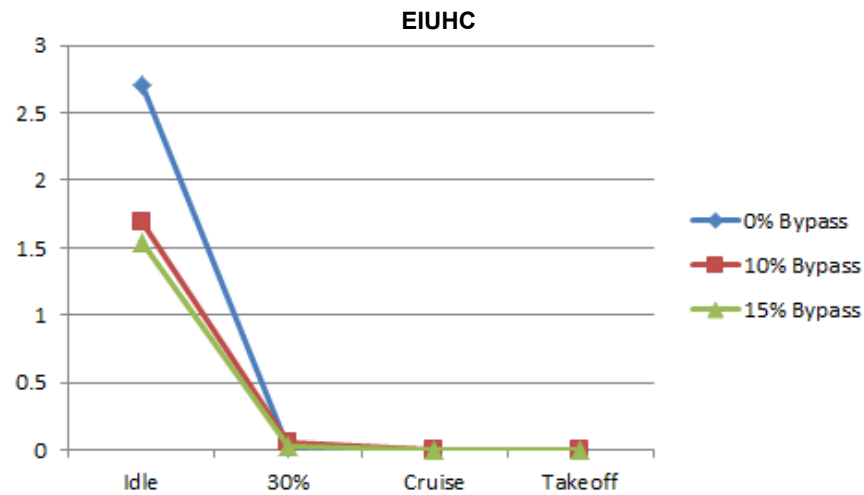Figure 53.—NOx emissions for full cycle at varying levels of TCLA.

Figure 54.—UHC emissions for full cycle at varying levels of TCLA.

TABLE 20.—EMISSIONS INDICES FOR FULL CYCLE AT VARYING LEVELS OF TCLA,
30 PERCENT POWER WITH ONLY PILOT-INTERMEDIATE CIRCUITS

TCLA, %	EICO				EINOx				EIHC			
	Idle	30%	Cruise	Takeoff	Idle	30%	Cruise	Takeoff	Idle	30%	Cruise	Takeoff
0	37.18	1.89	0.01	0.03	4.6	9.82	3.56	4	2.7	0.33	0	0
10	25.7	0.32	0.05	0.12	4.9	12.2	5.7	7.15	1.69	0.26	0	0
15	19.21	0.2	0.12	0.39	5	13.1	7.68	12.09	1.54	0.21	0	0

One unique factor to the system having three distinct circuits occurs at 30 percent power, where the system can either run with just pilot and intermediate or with all three circuits flowing. Swapping out the data for 30 percent power from the above charts (using all three circuits) and inserting the best result from the pilot-intermediate only scenario changes the overall cycle somewhat. Specifically, the pilot-intermediate 30 percent power case sees lower CO emissions, particularly with no bypass air, but has much higher NOx. Substituting this test point into the data yields Table 20 and Figure 55 to Figure 57. Note that only the 30 percent power case has been changed; all others remain identical to those shown above.
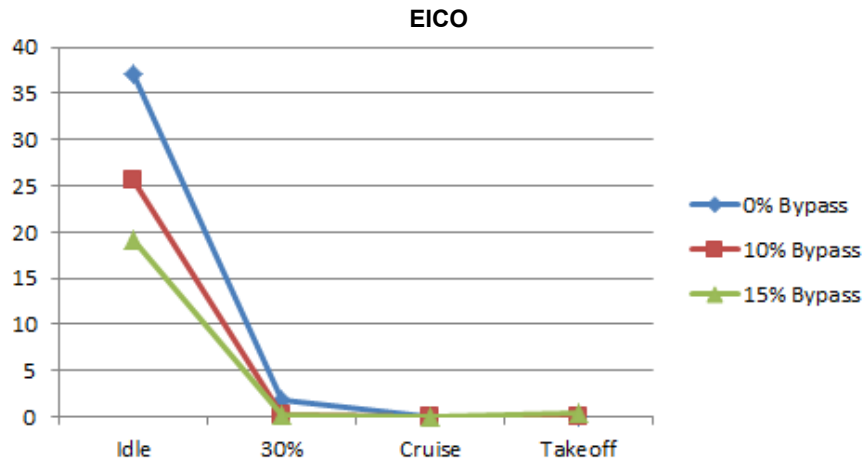
EICO

Figure 55.—CO emissions for full cycle at varying levels of TCLA, 30 percent power with only pilot-intermediate circuits.
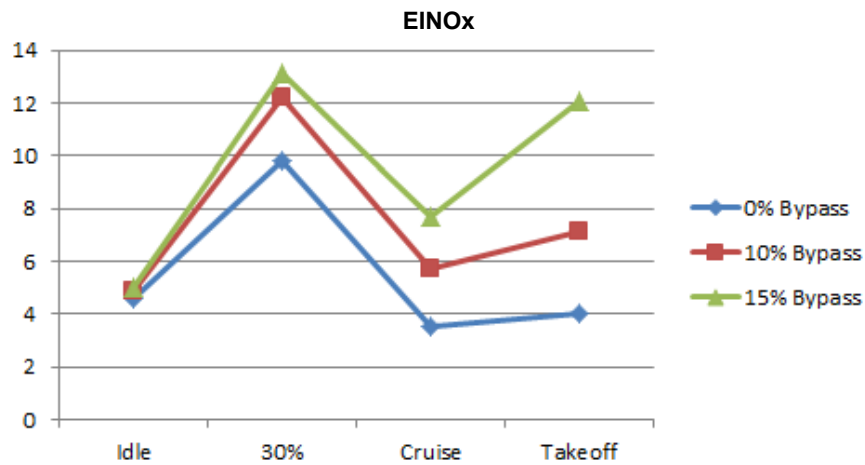
EINOx

Figure 56.—NOx emissions for full cycle at varying levels of TCLA, 30 percent power with only pilot-intermediate circuits.
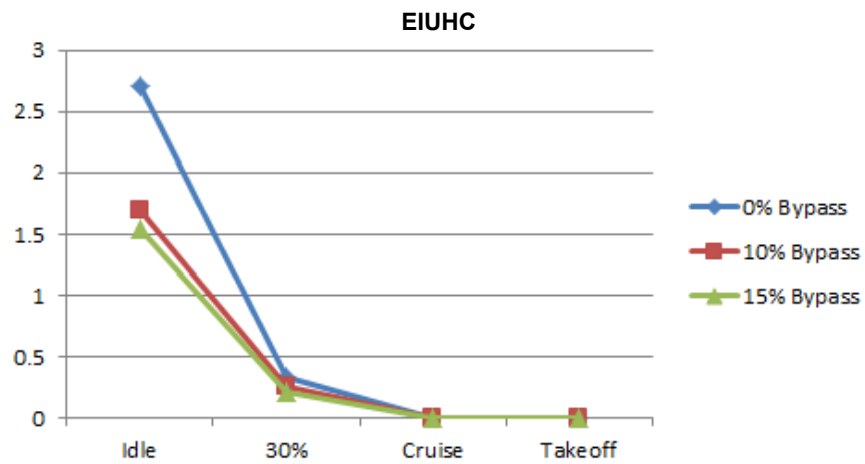
EIUHC

Figure 57.—UHC emissions for full cycle at varying levels of TCLA, 30 percent power with only pilot-intermediate circuits.

Clearly, there is a tradeoff at 30 percent power between CO and NOx emissions, depending on whether two or three circuits are lit. Possibly, given more time to test, some fuel split combination could be found that meets both criteria, but at a minimum it is clear that the UTAS design is capable of meeting either low CO or low NOx at 30 percent power.

Finally, some test data was recorded that did not correspond to the prescribed Pratt & Whitney boundary conditions. This information was useful for UTAS in evaluating other conditions at which the system could be operated as well as validation data for CFD. In the interest of completeness, this data is included in the report, in Table 21.

TABLE 21.—NON-DESIGN POINT TEST DATA

P3, psi	T3, °F	ΔP, %	Wf, p	Wf, i	Wf, o	Equivalent ratio, ϕ	FAR	EICO	EINOx	EIHC
77	510	3.55	42.1	21.1	0	0.23	0.016	184.29	3.42	N/A
200	720	3.03	68.7	101.7	0	0.27	0.018	38.79	8.31	N/A
210	720	2.86	44.7	124.1	0	0.26	0.018	36.68	7.17	N/A
211	721	3.06	23.8	146.8	0	0.26	0.018	57.6	6.47	N/A
209	721	3.08	17.6	144.6	0	0.25	0.017	98.94	5.83	N/A
220	993	3.45	55.1	55.1	61	0.26	0.017	2.89	4.82	0.52
219	998	3.5	42.9	51.1	66.1	0.24	0.016	33.69	2.74	0.25
222	1002	3.38	32.2	55.8	71.9	0.24	0.016	54.49	1.5	0.18
220	1002	3.41	32.3	63.4	65.3	0.24	0.017	29.78	1.56	0.14
219	1001	3.51	32.3	72.1	56	0.24	0.016	20.68	1.75	0.12
246	1002	3.42	37	84.2	64.2	0.24	0.016	21.28	1.91	0.08
232	1001	3.96	39.9	100.1	63.8	0.27	0.018	1.7	3.12	0.05
237	1001	3.83	32.2	103	105.1	0.32	0.022	0	2.39	0.04
246	1002	3.6	31.9	102.7	104.9	0.32	0.022	0	2.27	0.04
242	1036	4.26	32	102.6	104.5	0.3	0.02	0.01	1.78	0.03
242	1024	3.93	32.1	121.2	124.2	0.36	0.025	0.03	4.35	0.03
241	1023	3.78	29	125.3	128.3	0.38	0.026	0.05	5.48	0.02
244	1026	3.65	26	137.6	149.8	0.43	0.029	0.19	8.75	0.03
242	1026	3.55	20.9	140.3	152.4	0.43	0.029	0.2	8.74	0.02
238	1027	3.78	21.1	147	169.4	0.46	0.031	0.36	10.89	0.02
243	1030	4.07	19.7	147.7	168.3	0.43	0.03	0.17	8.2	0.01
248	1031	3.9	20.9	157	171	0.45	0.031	0.28	10.51	0.01
250	1030	3.58	21.4	163.4	197	0.51	0.035	0.86	17.74	0.01
199	724	3.29	25.7	64.8	65.7	0.24	0.016	753.34	1.13	N/A
210	718	2.77	33.9	89	86.1	0.33	0.023	2.13	2.38	3.17
203	714	2.97	27.4	87.7	89.1	0.32	0.022	7.42	1.56	0.7
202	713	3.02	34.1	96.1	73.6	0.32	0.022	8.13	2.66	0.5
212	713	3.14	33.6	96.5	73.6	0.3	0.021	69.43	2.03	N/A
212	712	3.16	34.1	96	73.5	0.3	0.021	33.8	2.15	N/A
196	710	2.98	33.9	96	73.4	0.34	0.023	1.55	3.31	N/A

Post Test CFD

The analysis of the data after completion of the test showed that the measured ACd (2.3 in^2) is high compared to the target nozzle ACd of 1.875 in^2). This is the result of air leakage, both around the individual nozzles, and around the rope seal between the dome plate and the array. Since the fuel ratio was determined by the overall air flow rate (which included all air leakage), the array was likely running richer at the local nozzle level than anticipated. To determine what effects this may have, CFD was re-run matching the rig test conditions, but with the addition of air along the top and bottom walls of the combustor, as shown in Figure 58. To maintain the same overall fuel air ratio, the additional fuel required was distributed through the injectors. As expected, the air from the leak did not mix adequately with the fuel from the nozzles within the intended mixing zones, and therefore the local fuel air ratio of the nozzles was higher (20 percent high). It is worth noting that these richer conditions are predicted to produce higher NOx as shown in Table 22. Future improvements in sealing these types of leaks are expected to show even further reductions NOx.
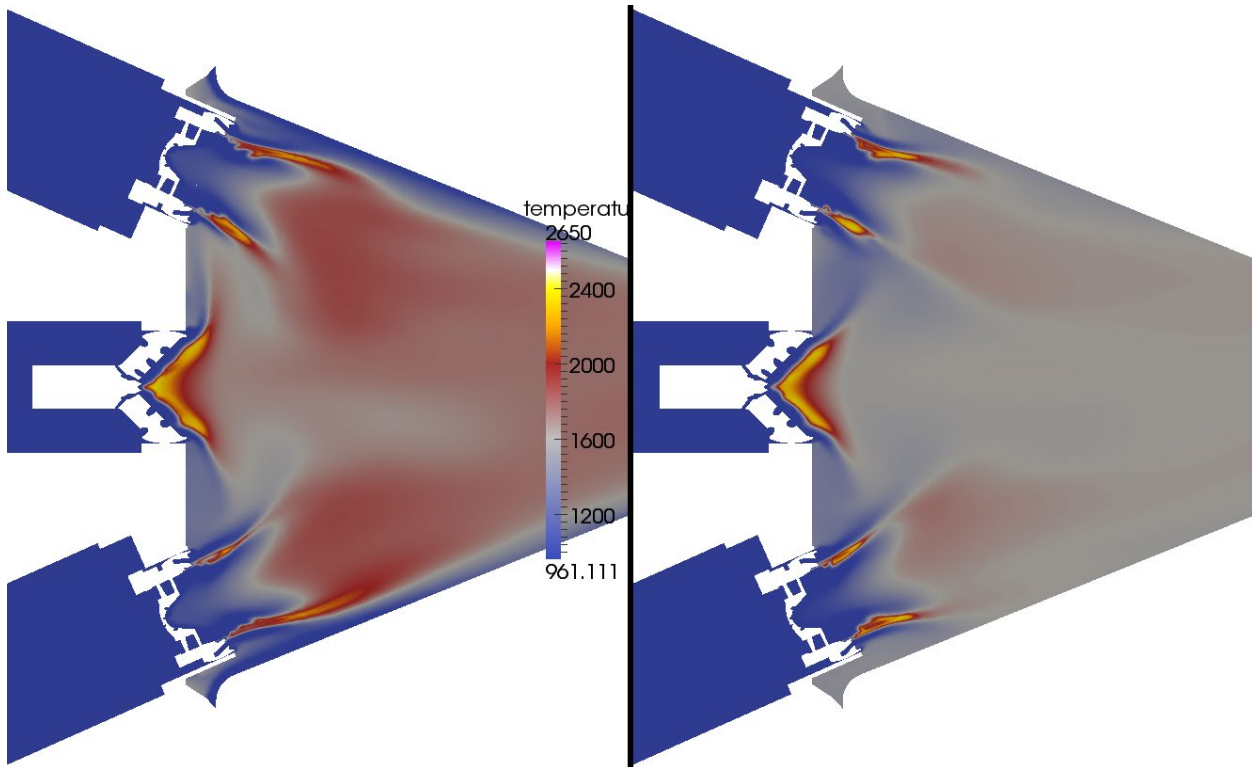

Figure 58.—CFD Contours of temperature with the approximated leak (left) and without leakage (right) at the same overall array FAR.

TABLE 22.—CFD PREDICTIONS OF EINOx

	P3, psi	T3, °F	Equivalence ratio, ϕ	CFD predicted EINOx, g-NOx/kg-fuel
Rig match point with leakage	250	1000	0.368	9.43
Rig match point without leakage	250	1000	0.368	5.02

Conclusions

This program successfully completed testing of a radially staged Multi-point Lean Direct Injection (MLDI) combustion system. The goal of this program was to use MLDI technology to demonstrate NOx reduction of 75 percent of the CAEP 6 recommendations in an advanced 55:1 pressure ratio gas turbine combustor environment. After extensive evaluation of design iterations using computational fluid dynamics rig testing at the UC indicated acceptable levels of ignition and LBO while testing in the CE-5 combustion rig at GRC indicated greater than 75 percent reduction in CAEP 6 NOx. In addition, the testing at NASA did not show significant levels of combustion instability at operating conditions.

Experimental results of the program included LBO at average FAR of 0.0046 using Jet-A fuel and 0.0044 using hydrotreated biofuel. Testing at NASA's CE-5 combustion rig resulted in best case EINOx at take-off conditions of less than 4 g-NOx/kg-fuel. All of the testing to date indicates that this system has acceptable levels of stability without any additional active or passive control. Evaluation of previous NASA emissions data indicates that 75 percent reduction in CAEP 6 NOx should achieve a maximum EINOx of 27 g-NOx/kg-fuel. Extrapolation of rig test data indicates the MLDI system should provide an EINOx of 26.8 g-NOx/kg-fuel at a fuel air ratio of 0.035 and a 55:1 pressure ratio. Thus this system is expected to meet, or exceed the objectives of this program. Evaluation of the rig test data also indicates that additional testing would, most likely, have provided improved results. The data shows a trend towards lower NOx with less fuel to the pilot which would be offset by more fuel going to the outer fuel injectors. Thus less fuel to the pilots would likely have resulted in lower emissions. This design incorporates a reduced number of injectors over previous multipoint designs, simplified and lightweight components, and a very compact combustor section. Additional outcomes of the program are validation that the design of these combustion systems can be aided by the use of Computational Fluid Dynamics to predict and reduce emissions. Furthermore, the staging of fuel through the individually controlled radially staged injector rows successfully demonstrated improved low power operability as well as improvements in emissions over previous multipoint designs. Additional comparison between Jet-A fuel and a hydrotreated biofuel is made to determine viability of the technology for use with alternative fuels. Finally, the operability of the array and associated nozzles proved to be very stable without requiring additional active or passive control systems. A number of publications have been published pertaining to this program along with three patent applications that have been submitted based on the unique technologies created during the course of this program.

1. REPORT DATE *(DD-MM-YYYY)*	2. REPORT TYPE	3. DATES COVERED *(From - To)*
01-04-2014	Final Contractor Report	

4. TITLE AND SUBTITLE
Multi-Point Combustion System
Final Report

5a. CONTRACT NUMBER
NNC11CA15C

5b. GRANT NUMBER

5c. PROGRAM ELEMENT NUMBER

6. AUTHOR(S)
Goeke, Jerry; Pack, Spencer; Zink, Gregory; Ryon, Jason

5d. PROJECT NUMBER

5e. TASK NUMBER

5f. WORK UNIT NUMBER
WBS 699959.02.26.03.04.05.09

7. PERFORMING ORGANIZATION NAME(S) AND ADDRESS(ES)
UTC Aerospace Systems
811 4th Street
West Des Moines, Iowa 50265

8. PERFORMING ORGANIZATION REPORT NUMBER
E-18851

9. SPONSORING/MONITORING AGENCY NAME(S) AND ADDRESS(ES)
National Aeronautics and Space Administration
Washington, DC 20546-0001

10. SPONSORING/MONITOR'S ACRONYM(S)
NASA

11. SPONSORING/MONITORING REPORT NUMBER
NASA/CR-2014-218112

12. DISTRIBUTION/AVAILABILITY STATEMENT
Unclassified-Unlimited
Subject Category: 07
Available electronically at http://www.sti.nasa.gov
This publication is available from the NASA Center for AeroSpace Information, 443-757-5802

13. SUPPLEMENTARY NOTES

14. ABSTRACT
A low-NOx emission combustor concept has been developed for NASA's Environmentally Responsible Aircraft (ERA) program to meet N+2 emissions goals a 75 percent reduction of LTO NOx from CAEP6 standards without increasing CO, UHC, or smoke from that of current state of the art. The design, analysis, and test of a multi-point combustion system are described. All design work was based on the results of Computational Fluid Dynamics modeling with the end results tested on a medium pressure combustion rig at the UC and a medium pressure combustion rig at GRC. The design incorporates a reduced number of injectors over previous multipoint designs, simplified and lightweight components, and a very compact combustor section. The staging of fuel through the individually controlled radially staged injector rows successfully demonstrated improved low power operability as well as improvements in emissions over previous multipoint designs. Additional comparison between Jet-A fuel and a hydrotreated biofuel is made to determine viability of the technology for use with alternative fuels. Finally, the operability of the array and associated nozzles proved to be very stable without requiring additional active or passive control systems.

15. SUBJECT TERMS
Gas turbines; Injectors; Nitrous oxide

16. SECURITY CLASSIFICATION OF:			17. LIMITATION OF ABSTRACT	18. NUMBER OF PAGES	19a. NAME OF RESPONSIBLE PERSON
a. REPORT	b. ABSTRACT	c. THIS PAGE			STI Help Desk (email:help@sti.nasa.gov)
U	U	U	UU	44	19b. TELEPHONE NUMBER *(include area code)* 443-757-5802